

# Overconfidence in climate overshoot

Carl-Friedrich Schleussner<sup>1,2,3</sup>, Gaurav Ganti<sup>1,2,3</sup>, Quentin Lejeune<sup>1,2</sup>, Biqing Zhu<sup>4</sup>, Peter Pfleiderer<sup>1,5</sup>, Ruben Prütz<sup>2,6</sup>, Philippe Ciais<sup>4</sup>, Thomas L. Frölicher<sup>7,8</sup>, Sabine Fuss<sup>2,6</sup>, Thomas Gasser<sup>3</sup>, Matthew J. Gidden<sup>1,3</sup>, Chahan M. Kropf<sup>9,10</sup>, Fabrice Lacroix<sup>7,8</sup>, Robin Lamboll<sup>11</sup>, Rosanne Martyr-Koller<sup>1,2</sup>, Fabien Maussion<sup>12</sup>, Jamie W. McCaughey<sup>9,10</sup>, Malte Meinshausen<sup>3,13,14</sup>, Matthias Mengel<sup>15</sup>, Zebedee Nicholls<sup>3,13,14</sup>, Yann Quilcaille<sup>9</sup>, Benjamin Sanderson<sup>16</sup>, Sonia Seneviratne<sup>9</sup>, Jana Sillmann<sup>5</sup>, Christopher J. Smith<sup>3,17,18</sup>, Norman J. Steinert<sup>16</sup>, Emily Theokritoff<sup>1,2</sup>, Rachel Warren<sup>19</sup>, Jeff Price<sup>19</sup>, Joeri Rogelj<sup>3,20</sup>

<sup>1</sup> Climate Analytics, Berlin, Germany

<sup>2</sup> Geography Department and IRITHESys Institute, Humboldt-Universität zu Berlin, Berlin, Germany

<sup>3</sup> International Institute for Applied Systems Analysis (IIASA), Laxenburg, Austria

<sup>4</sup> Laboratoire des Sciences du Climat et de l'Environnement LSCE, Orme de Merisiers, Gif-sur-Yvette, France

<sup>5</sup> University of Hamburg, Research Unit for Sustainability and Climate Risks, Hamburg, Germany

<sup>6</sup> Mercator Research Institute on Global Commons and Climate Change (MCC), Berlin, Germany

<sup>7</sup> Climate and Environmental Physics, Physics Institute, University of Bern, Switzerland

<sup>8</sup> Oeschger Centre for Climate Change Research, University of Bern, Switzerland

<sup>9</sup> Department of Environmental Systems Science, ETH Zürich, Zürich, Switzerland

<sup>10</sup> Federal Office of Meteorology and Climatology MeteoSwiss, Zürich, Switzerland

<sup>11</sup> Centre for Environmental Policy, Imperial College London, UK

<sup>12</sup> Department of Atmospheric and Cryospheric Sciences, University of Innsbruck, Innsbruck, Austria

<sup>13</sup> School of Geography, Earth and Atmospheric Sciences, The University of Melbourne, Melbourne, Australia

<sup>14</sup> Climate Resource, Melbourne, Victoria, Australia

<sup>15</sup> Potsdam Institute for Climate Impact Research, Potsdam, Germany

<sup>16</sup> CICERO, Oslo, Norway

<sup>17</sup> Met Office Hadley Centre, Exeter, UK

<sup>18</sup> School of Earth and Environment, University of Leeds, UK

<sup>19</sup> Tyndall Centre for Climate Change Research and School of Environmental Sciences, University of East Anglia, Norwich, UK

<sup>20</sup> Grantham Institute for Climate Change and the Environment and Centre for Environmental Policy, Imperial College London, London, UK

*Global emission reduction efforts continue to be insufficient to meet the temperature goal of the Paris Agreement<sup>1</sup>. This makes the systematic exploration of so-called overshoot pathways that temporarily exceed a targeted global warming limit before drawing temperatures back down to safer levels a priority for science and policy<sup>2-5</sup>. Here, we show that global and regional climate change and associated risks after an overshoot are substantially different from a world that avoids it. We find that achieving declining global*

*temperatures can limit long-term climate risks compared to a mere stabilisation of global warming, including for sea-level rise and cryosphere changes. However, the possibility that global warming could be reversed many decades into the future is of limited relevance for adaptation planning today. Temperature reversal may be undercut by strong Earth-system feedbacks resulting in high near-term and continuous long-term warming<sup>6,7</sup>. To hedge and protect against high-risk outcomes, we identify the geophysical need for a preventive carbon dioxide removal capacity of several hundred gigatonnes. Yet, technical, economic and sustainability considerations may limit CDR deployment at such scales<sup>8,9</sup>. We thus cannot be confident that temperature decline after overshoot is achievable. Only rapid near-term emission reductions are effective in reducing climate risks.*

The possibility of surpassing and subsequently returning below dangerous levels of global warming has been a topic of discussion for decades<sup>10</sup> with large-scale carbon dioxide removal (CDR) identified early on as playing a key role in such temperature reversal<sup>11,12</sup>. Since the adoption of the Paris Agreement in 2015 the issue has risen to further prominence.

The temperature goal of the Paris Agreement allows for some ambiguity in its interpretation but establishes 1.5°C as the long-term upper limit for global temperature increase<sup>13,14</sup>. This means that if 1.5°C is temporarily exceeded (referred to as an overshoot), a reversal of warming is part and parcel of meeting the Paris Agreement's long-term ambition<sup>13</sup>. In addition, the Paris Agreement text does not indicate that temperature must stabilise but instead establishes upper limits below which temperatures must peak and can then decline. This understanding is further strengthened by looking at other, specific goals in the Paris Agreement. Indeed, achieving global net-zero greenhouse gas (GHG) emissions as implied by Article 4.1 of the Paris Agreement would in the median estimate lead to declining temperatures in the long term<sup>6,13</sup>.

Global greenhouse gas (GHG) emission pathways play a central role in informing the development of policy benchmarks in line with the Paris Agreement and are a core part of climate change assessments by the Intergovernmental Panel on Climate Change (IPCC)<sup>2,15</sup>. Such assessments categorise pathways based on their maximum temperature outcome<sup>2,15</sup>. Because a peak and gradual reversal of global warming turns out to be a fundamental feature of Paris-compatible pathways<sup>16</sup>, we propose to henceforth categorise pathways in terms of their peak and decline characteristics (Table 1).

Peak-and-decline (PD) pathways are differentiated by the stringency of emission reduction efforts in the near term and up to achieving net-zero CO<sub>2</sub> emissions and the assumed net-negative CO<sub>2</sub> emissions in the long term<sup>16</sup>. The former determines the maximum cumulative CO<sub>2</sub> emissions of a pathway and thereby approximately the magnitude and time of peak warming for median climate outcomes<sup>6,16</sup>. The latter determines the pace of potential temperature reversal<sup>16</sup>. Both aspects are further influenced by non-CO<sub>2</sub> emissions.

Several categories of PD pathways have been proposed in the scientific literature<sup>2,17</sup> (Table 1). A prominent example is the latest Working Group III (WGIII) contribution to the IPCC Sixth Assessment Report (AR6), which includes two pathway categories explicitly referring to the term overshoot (Table 1). Temperature overshoot pathways are a sub-category in the peak-and-decline categorisation we present here, with the distinguishing characteristic of these pathways being that their intended maximum temperature limit (e.g. 1.5°C) is temporarily exceeded.

Although defined in terms of probabilities of temporarily exceeding 1.5°C, the IPCC AR6 scenario categories frame a possible overshoot quite concretely: limited overshoot (C1) refers to exceeding the specified limit by up to about 0.1°C, while high overshoot (C2) refers to exceeding it by more than 0.1°C and up to 0.3°C<sup>2,15</sup> (Table 1). This naming and framing suggests that temperature overshoots in these pathway categories are constrained to a few tenths of a degree with high certainty. This is not the case. Because the overshoot numbers refer to median warming, substantially higher warming outcomes are distinctly possible - as we will show below. A strong focus on median outcomes might lead to overconfidence in the perception of the risks implied by overshoot pathways.

In the following, we provide a comprehensive perspective on future climate outcomes under PD pathways (see Table 1 and Fig 1 for a conceptual overview). We explore the uncertainties in global temperature outcomes and their implications for the required net-negative CO<sub>2</sub> emissions to achieve the intended reversal of warming. We then discuss feasibility and sustainability constraints of deploying gigatonne-scale CDR. Next, we explore if and how global mean temperature reversal translates into the reversal of climatic impact drivers<sup>6</sup> and subsequent impacts and risks. Finally, we discuss the implications of considering or experiencing temperature overshoot for climate change adaptation. Based on this comprehensive perspective, we argue for redirecting the discussion towards reducing climate risks both in the near and long-term, and to avoid overconfidence in the possibility, well-behaved characteristics and desirability of climate overshoot.

**Table 1 | Conceptual and literature categories of peak and decline emission pathways.**

Pathway Category		Temperature Characteristics	Emission Characteristics (Best Estimates)
<b>Conceptual Categories</b>			
PD: Peak and decline pathways		Pathways that aim to achieve temperature peak and a sustained long-term temperature decline of at least several decades in duration	Emission reductions in all GHGs towards achieving net-zero CO2 emissions, and net-negative CO2 emissions thereafter
	<b>PD-OS:</b> Overshoot pathways	PD-pathways that aim to limit warming to a targeted warming level at some point in the far future but allow it to be exceeded with high likelihood over the near term in the conviction that warming can be reversed at a later stage to again land below the targeted limit	As peak and decline pathways, but rate of emission reduction, timing of net-zero CO2 and amount of net-negative emissions depend on the characteristics of the envisaged overshoot
	<b>PD-EP:</b> Enhanced protection pathways	PD-Pathways that aim to keep peak global warming as low as possible and gradually reverse warming thereafter to reduce climate risks	Stringent and rapid GHG emission reduction to reduce emissions as much and as early as possible, achieving net-zero CO2 emissions as soon as possible while minimising residual emissions, and achieving sustainable levels of net-negative CO2 emissions thereafter in order to potentially reach net-zero or net-negative GHGs.
<b>Literature Categories</b>			
Pathways that limit warming to 1.5°C (>50%) with no or limited overshoot (C1) <sup>2</sup>		<p>Pathways that limit warming to 1.5°C in 2100 with a likelihood of greater than 50%, and reach or exceed warming of 1.5°C during the 21st century with a likelihood of 67% or less.</p> <p>Limited overshoot refers to exceeding 1.5°C global warming by up to about 0.1°C and for up to several decades. C1 pathways that achieve net-zero GHG are included in the category C1a.</p>	<p>2030 reductions of total GHG emissions relative to 2019: 43% [34-60 %, 5th-95th percentile range]</p> <p>Timing of net-zero CO2: 2050-2055 [2035-2070]</p> <p>Timing of net-zero GHG (only category C1a pathways): 2070-2075 [2050-2090]</p> <p>Cumulative net-negative CO2 after net-zero: 220 GtCO<sub>2</sub> [20-660]</p>
Pathways that return warming to 1.5°C (>50%) after a high overshoot (C2) <sup>2</sup>		<p>Pathways that limit warming to 1.5°C in 2100 with a likelihood of greater than 50%, and exceed warming of 1.5°C during the 21st century with a likelihood of greater than 67%.</p> <p>High overshoot refers to temporarily exceeding 1.5°C global warming by 0.1-0.3°C for up to several decades</p>	<p>2030 reductions of total GHG emissions relative to 2019: 23% [0-44 %, 5th-95th percentile range]</p> <p>Timing of net-zero CO2: 2055-2060 [2045-2070]</p> <p>Timing of net-zero GHG: 2070-2075 [2055-...]</p> <p>Cumulative net-negative CO2 after net-zero: 360 GtCO<sub>2</sub> [60-680]</p>

<p>Paris Agreement compatible pathways<sup>17</sup></p>	<p>Pathways that reach or exceed warming of 1.5°C during the 21st century with a likelihood of 67% or less, and simultaneously do not exceed 2°C during the 21st century with a likelihood of 90% or more.</p> <p>Achieve long-term declining temperature by reaching net-zero GHGs. Similar to pathways in category C1a.</p>	<p>2030 reductions of total GHG emissions relative to 2019: 41% [38-44 %, interquartile range]</p> <p>Timing of net-zero CO2: 2050 [2045-205]</p> <p>Timing of net-zero GHG: 2065 [2060-2075]</p> <p>Cumulative net-negative CO2 after net-zero: 453 GtCO<sub>2</sub> [127 - 690]</p>
---	---	---

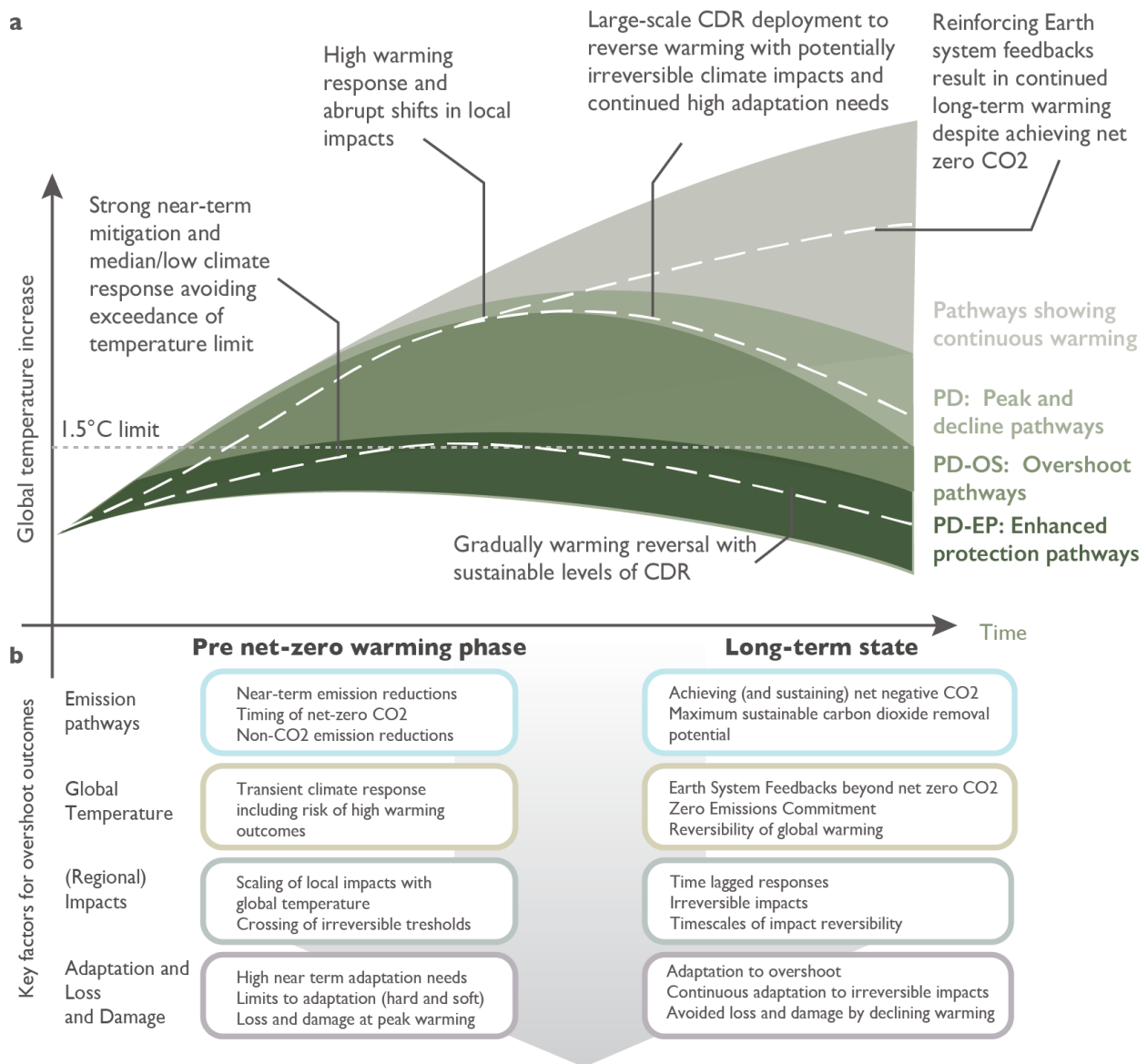


**Fig 1 | Illustrative climate outcomes under different conceptual categories of overshoot pathways. a,** Different classes of peak and decline global mean temperature pathways (compare Table 1). Stylised individual pathways (dashed lines) are highlighted to illustrate specific impact, adaptation and carbon dioxide removal dimensions associated with the different categories. **b,** An overview of key factors affecting pathway and potential overshoot outcomes along the impact chain for the warming phase until net-zero CO<sub>2</sub> and for the long term beyond net-zero.

## Global climate response uncertainty and reversal

Peak warming increases with increasing cumulative CO<sub>2</sub> emissions till global net zero CO<sub>2</sub> and less stringent reductions in non-CO<sub>2</sub> greenhouse gases. Achieving net-negative CO<sub>2</sub> emissions (NNCE) after peak warming can result in a long-term decline in warming<sup>6</sup>. Most estimates of the NNCE consistent with a long-term reversal of warming in PD pathways have focused on median long-term warming outcomes<sup>15</sup>. However, to comprehensively assess overshoot risks and the NNCE requirements for warming reversal in PD pathways, also uncertainties in the climate response must be considered. These include uncertainties during the warming phase (e.g., high warming outcomes due to amplifying warming feedbacks)<sup>18</sup> and in the long-term state (potential for continued warming post net-zero CO<sub>2</sub> and the response of the climate system to NNCE)<sup>7</sup>.

We explore NNCE requirements for an illustrative pathway with the following characteristics (Fig. 2a): (1) it achieves net zero CO<sub>2</sub> around mid-century, (2) limits median peak warming close to 1.5°C above pre-industrial levels, and (3) has no NNCE. We use 2237 calibrations of the simple carbon cycle and climate model FaIR v1.6.2 to estimate the range of physically plausible warming outcomes for this pathway, consistent with the uncertainty assessment of IPCC AR6 (Fig. 2a, Methods). Two groups of plausible futures stand out. The first includes relatively low-risk futures where warming peaks below 1.5°C at or before net zero CO<sub>2</sub> (Fig. 2b, bottom left quadrants); in these cases, NNCE is not required. We also identify relatively high-risk futures where warming exceeds 1.5°C at net zero CO<sub>2</sub> and continues beyond (Fig. 2b, top right quadrant).

For each respective FaIR calibration, we estimate the NNCE required to return warming to 1.5°C in 2100 (Methods). We find that a need for large NNCE deployment cannot be ruled out to ensure warming is halted, due to the heavy-tailed climate response uncertainty distribution<sup>18</sup> (Fig. 2c). The scale of this deployment (interquartile range: 0 to -400 Gt CO<sub>2</sub> cumulatively until 2100, or, 0 to -10 Gt CO<sub>2</sub>/yr after 2060) is of the same order of magnitude as the spread of deployed NNCE across the scenarios assessed in IPCC AR6 WGIII (Fig. 2c). Although we find that NNCE requirements resulting from a higher-than-average peak warming due to a strong transient climate response dominate, cumulative NNCE until 2100 of up to 200 Gt CO<sub>2</sub> (or -5 Gt CO<sub>2</sub>/yr, upper 95% quantile, Fig. 2c) could be required to hedge against further warming past net-zero<sup>19</sup>. Our results show that a narrow focus on scenario uncertainty and median warming alone is insufficient to assess potential CDR deployment requirements even for merely achieving a stable global temperature in the 21st century.

CDR requirements here refer to additional carbon removal due to anthropogenic activity in line with the conventions and definitions of the models underlying our assessment. It is important to note that parties to the UNFCCC use a different definition for defining land-based carbon fluxes, which results in a ~4-7 Gt CO<sub>2</sub>/yr difference between national GHG inventories and scientific models that needs to be considered when translating these insights into policy advice<sup>20</sup>.

Our simple illustrative approach has a number of limitations that would benefit from further exploration, including with dedicated state-of-the-art Earth system model (ESM)<sup>21</sup>. Particularly relevant questions arise around issues of asymmetry in the response of the climate system to positive and negative CO<sub>2</sub> emissions (Methods)<sup>22,23</sup>. We note that due to the lack of appropriate training data, the response of simple climate models to NNCE is not well constrained. Moreover, the ESMs used to calibrate simple climate models may miss non-linear responses in the climate system including abrupt destabilisation of natural carbon sinks<sup>24</sup> (e.g., permafrost CO<sub>2</sub> and CH<sub>4</sub> release, peat carbon loss from climate change and degradation or conversion of peatland, extreme fires and drought mortality of forests). We explore permafrost and peatland responses to overshoot below (Fig. 4).

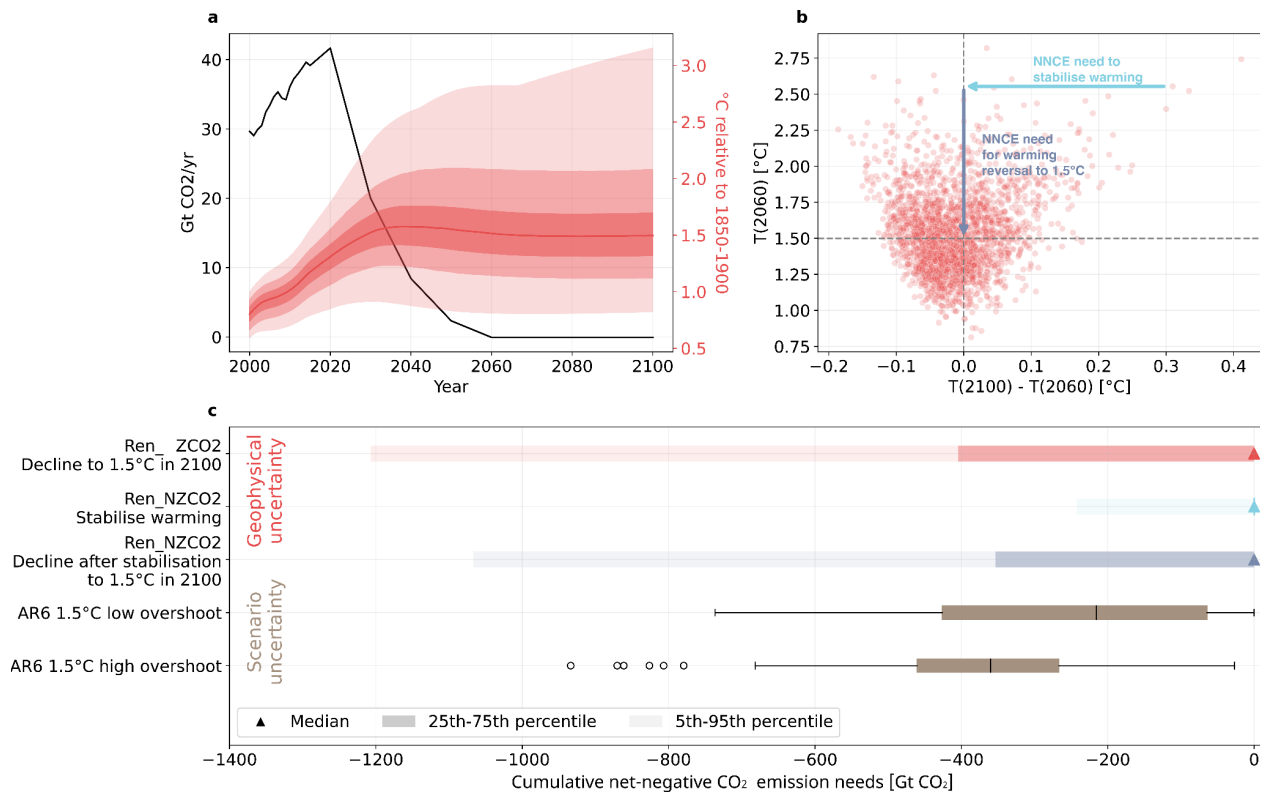


**Figure 2 | Estimating cumulative net-negative CO<sub>2</sub> emissions (NNCE) needs when accounting for climate response uncertainty. a**, Net CO<sub>2</sub> emissions for the PROVIDE REN\_NZCO2 pathway (black line) and the warming outcome uncertainty (derived using FaIR v1.6.2, Methods). The median warming outcome is the red solid line, with each subsequent plume of varying transparency representing, in order, the 25th - 75th percentile, 5th - 95th percentile, and minimum to maximum ranges respectively. **b**, Peak warming at the time of net-zero CO<sub>2</sub> (2060) versus the change in temperature between net-zero CO<sub>2</sub> and 2100. **c**, Estimated NNCE to return warming for each peak warming outcome shown in **b** to 1.5°C in 2100 (Methods). These estimates reflect NNCE implied by geophysical uncertainty of the warming outcome based on the REN\_NZCO2 pathway and are compared to the scenario uncertainty across the C1 and C2 categories from the IPCC AR6 WGIII report that is implied by considering median estimates of the geophysical response to emissions.

## **Relying on Carbon Dioxide Removal**

Achieving NNCE will require the deployment of CDR that exceeds residual emissions in hard-to-abate sectors. Pathways assessed by IPCC WGIII deploy CDR in different ways and to different extents<sup>3</sup>. Scale-up of CDR is most rapid in pathways with the lowest peak warming (low or no overshoot 1.5°C pathways, C1, Extended Data Fig. 3). Across the ensemble of emission pathways, CDR levels by the end of the century are generally higher in high overshoot C2 pathways, but the full (5-95%) range is similar to the C1 pathways range. Pathways that keep warming below 2°C, but do not limit warming to 1.5°C in 2100 (C3) see a substantial CDR ramp-up in the second half of the 21st century reaching levels comparable to C1 pathways by 2080 (Extended Data Fig. 3). The total CDR amount deployed in pathways until 2100 depends predominantly on the effective reduction of residual positive CO<sub>2</sub> emissions and mitigation of non-CO<sub>2</sub> GHGs<sup>17</sup>.

In the previous section we showed how the extent of CDR required to achieve stable temperatures in the 21st century might be strongly underappreciated. Here we highlight that there are multiple areas where current pathways might be overconfident in their assumed use of CDR (Extended Data Table 1). Upscaling of CDR may be constrained considerably<sup>9</sup> by factors such as lack of policy support and business models, technological uncertainty and public opposition (e.g., perceived risks of delaying mitigation<sup>25</sup>). Even if technical removal potentials prove to be large, sustainability and equity considerations would limit acceptable deployment scales<sup>8,9</sup>. Insufficient technological readiness may be a critical bottleneck, as current removal rates from CDR methods other than afforestation and reforestation are minuscule (~2 Mt CO<sub>2</sub>/yr)<sup>26</sup> and would require a more than 1000-fold increase by 2050<sup>8</sup>. Beyond technological concerns, an array of unintended or uncertain permanence issues and system feedbacks (Extended Data Table 1) might reduce or offset CDR's contribution to mitigation<sup>26,27</sup>.

Squaring these feasibility concerns with the potential need for gigatonne-scale CDR deployment to address climate uncertainty (Fig. 2) will be challenging. We argue that deployment pathways that address this challenge should be guided by the principle of harm prevention<sup>28</sup> under enhanced protection pathways (PD-EP, Table 1). This approach requires two complementary actions: (1) reduce gross CO<sub>2</sub> emissions rapidly to reduce the total CDR requirements, and (2) address feasibility concerns to facilitate the deployment of net-negative CDR to hedge against potentially high warming outcomes.

## **Regional climate change reversibility**

The proposition of overshoot pathways is that failure to keep warming below a desired temperature limit is accepted under the promise that global warming is returned back below a certain level, i.e. 1.5°C, in the long run. Since this climate overshoot narrative is focused on what happens to global mean temperatures, it leads to the impression that achieving a climate objective after an overshoot is just a different trajectory to arrive at the same endpoint. Yet, this is not necessarily the case for regional climatic changes, and understanding the implications of a global temperature overshoot for regional changes is critical.

We explore this question with dedicated modelling simulations comparing overshoot and long-term stabilisation in two ESMs and find substantial differences in regional climate impact drivers on multi-century timescales (Fig. 3, Extended Data Fig. 4, Methods). Strong regional features emerge over the high northern latitude oceans as a result of a time-lagged response of the Atlantic Meridional Overturning Circulation (AMOC)<sup>4,29</sup>. In the NorESM2-LM model, we observe a reversal of regional temperature scaling with GMT change for the North Atlantic and adjacent European land regions under overshoot (Fig. 3c), leading to a temporary regional cooling and a subsequent regional recovery and warming (Fig. 3d)<sup>30</sup>. We note that these simulations do not include increased Greenland meltwater influx that may suppress a potential AMOC recovery under overshoot<sup>31</sup>. The pattern where the North Atlantic regionally cools despite planetary warming is also present in the stabilisation scenario, but less pronounced. In the GFDL-ESM2M model, the imprint of overshoot and stabilisation on regional climate is less drastic. But a time-lagged AMOC recovery about 100 years after peak warming and to higher levels than in the stabilisation scenario is also apparent (Fig. 3d,f). Similarly pronounced features emerge for precipitation in both models, in particular on the regional level related to movements of the Inter-Tropical Convergence Zone (ITCZ) in response to changes in the AMOC<sup>4</sup> (Extended Data Fig. 4). Multi-model simulations corroborate the finding that AMOC dynamics and related changes in regional climate are a dominant feature of transient overshoot simulations (Method, Extended Data Fig. 6,7)<sup>5,30</sup>. They also indicate a continuous warming of the Southern Ocean relative to the rest of the globe as a result of fast and slow response patterns<sup>32</sup>, and changes in regional climate following reduced aerosol loadings (in particular in South and East Asia)<sup>18</sup>. Indeed, even if global warming is stabilised at a certain level without overshoot, the climate system continues to change as its components keep adjusting and equilibrate<sup>33</sup>. Taken together, our results indicate that regional climate changes cannot be approximated well by GMT after peak warming.

We find substantial long-term imprints of overshoot on regional climate (Fig. 3c,d) that are distinct from transient changes in stabilisation scenarios (Extended Data Fig. 5). However, substantial differences in model dynamics (compare Fig. 3e,f) remain, pointing towards high risks and low confidence in the exact behaviour that can be expected. Dedicated multi-model experiments would be required to further investigate the long-term consequences of overshoot compared to stabilisation<sup>21</sup>.

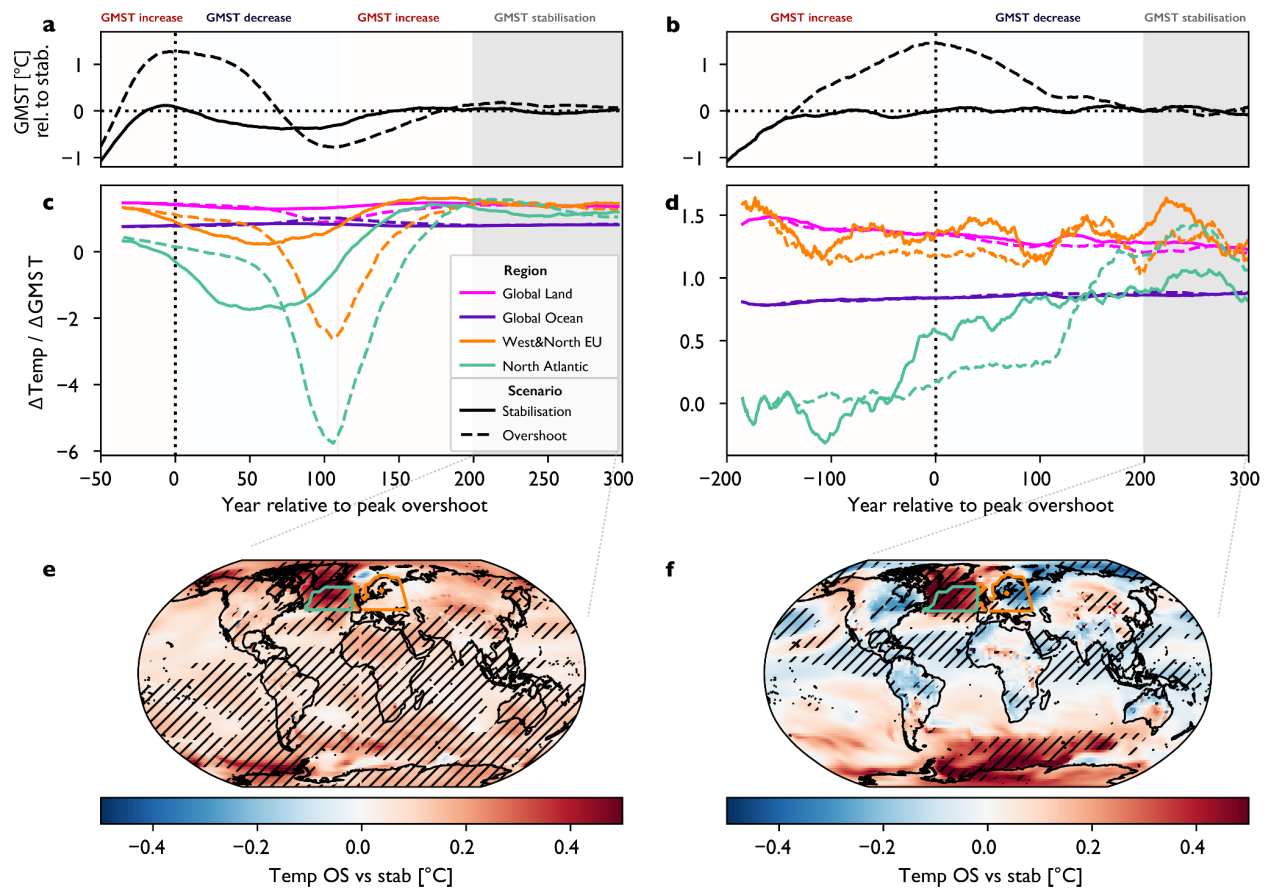


**Fig 3 | Evolution of regional temperatures before and after overshoot compared to global temperature stabilisation. a,c,e** show results for the NorESM Earth System Model, **b,d,f** for GFDL-ESM2M. **a,b** Global mean surface air temperature (GMT) trajectories for dedicated climate stabilisation (solid) and overshoot (dashed) scenarios. **c,d** temporal evolution of scaling coefficients of annual regional temperatures with GMT for the global land and ocean areas as well as the North Atlantic Ocean (north of 45°N) and Western and Northern Europe. **e,f** regional differences in annual temperature between overshoot and stabilisation scenarios over one hundred years of long-term GMT stabilisation (grey shaded area in panels **a,b**, hatching highlights grid-cells where the difference exceeds the 95th percentile (is below the 5th percentile) of comparable period differences in piControl simulations (see Methods).

### **Time-lagged and irreversible impacts**

For a range of climate impacts, there is no expectation of immediate reversibility after overshoot. This includes changes in the deep ocean, marine biogeochemistry and species<sup>34</sup>, land-based biomes, carbon stocks and crop yields<sup>35</sup>, but also biodiversity on land<sup>36</sup>. An overshoot will also increase the probability of triggering potential Earth system tipping elements<sup>31</sup>. Sea levels will continue to rise for centuries to millennia even if long-term temperatures decline<sup>37</sup>.

Comprehensively assessing future climate risks under PD pathways requires not only a focus on the (irreversible) consequences of a temporary overshoot, but also on the benefits of long-term temperature reversal, compared to stabilisation at higher levels. Here we explore the consequences of overshoot in an ensemble of PD pathways (Methods) that achieve net-zero GHGs and thereby long-term temperature decline, compared to stabilisation at peak warming (by maintaining net-zero CO<sub>2</sub>).

For global sea-level rise, we find that every 100 years of overshoot above 1.5°C lead to an additional sea-level rise commitment of around 40 cm by 2300 (central estimate) relative to a baseline of about 80 cm without overshoot (Fig. 4a). For high-risk outcomes, the 2300 sea-level rise commitment could be about 3 times (95% percentile) above the central estimate (Extended Data Fig. 9)<sup>37</sup>. Long-term temperature decline at about 0.03-0.04°C per decade (net-zero GHGs) avoids about 40 cm of 2300 sea-level rise (median estimate, 95% percentile about 1.5m) compared to stabilisation at peak warming (Fig. 4b).

A similar pattern emerges for 2300 permafrost thaw and northern peatland warming leading to increased soil carbon decomposition and CO<sub>2</sub> and CH<sub>4</sub> release (Fig.4, Extended Data Fig. 8). The effect of permafrost and peatland emissions on 2300 temperatures increases by 0.02°C per 100 years of overshoot, while achieving long-term declining temperatures would reduce the additional 2300 temperature effect by about 0.017°C. We caution that the diagnosed linear relationship between overshoot length and impact outcome may depend on the set of pathways that it was derived from. The underlying pathways assume overshoots starting from a period of delay in climate action followed by a steady reduction to net zero GHG emissions implying a similar rate of long-term temperature decline in all pathways. The relationship could be different for more, or less extreme overshoot outcomes.

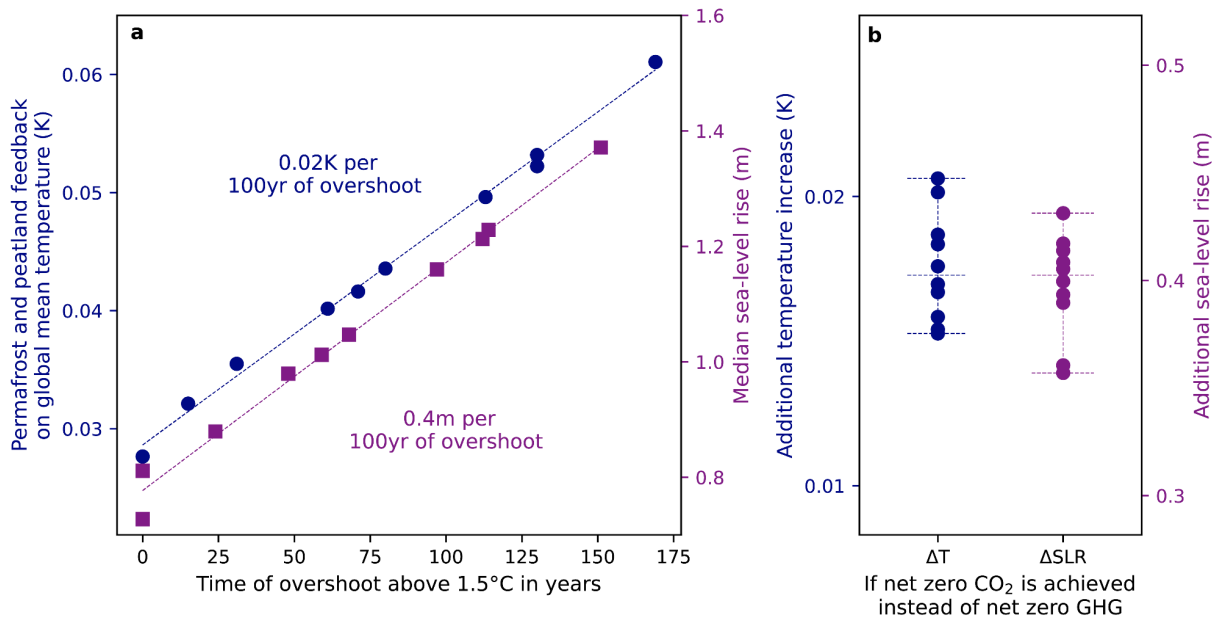


**Fig 4 | Long-term irreversible permafrost, peatland and sea-level rise impacts of overshoot. a,** Feedback on 2300 global mean temperature increase by permafrost and peatland emissions (blue markers and left axis) and 2300 global median sea-level rise (right axis) as a function of overshoot duration. **b,** Additional global mean temperature from warming-induced permafrost and peatland emissions and sea-level rise increase implied by stabilising temperatures at peak warming by achieving net-zero CO<sub>2</sub> emissions compared to a long-term temperature decline implied by achieving and maintaining net-zero GHGs.

### Socio-economic impacts

The severity of climate risks for human systems under overshoot will significantly depend on their adaptive capacity<sup>38</sup>, as well as the potential transgression of limits to adaptation<sup>39</sup>. An overshoot above 1.5°C would likely emerge during the first half of the 21st century, a period still characterised by comparably low adaptive capacity in large parts of the globe even under optimistic scenarios of socio-economic development<sup>38</sup>. The coincidence of overshoot and low adaptive capacity can amplify climate risks. This has profound consequences for the ability to achieve climate-resilient and equitable development outcomes under overshoot in particular for the most vulnerable countries, communities and peoples.

Climate impacts on health, mortality, ecosystem services, livelihoods, and education can leave lasting and intergenerational negative effects on people's well-being<sup>40</sup>. Overshoots might also leave a long-term legacy in the economic performance of countries, in particular the world's poorest, due to suggested impacts of climate change on economic growth<sup>41</sup>.

Therefore, overshoot entails deeply ethical questions of how much additional climate-related loss and damage people, and especially the world's poor, would need to endure.

### **Adaptation decision-making and overshoot**

In contrast with the prominence of overshoot pathways in the mitigation literature, their implications for adaptation planning have not been widely explored<sup>42</sup>. It poses the question of whether the possibility of impact reversal in the long-term future is relevant for today's adaptation planning. This is a question of timescales.

Even under the optimistic assumption of nearly full reversibility of a climate impact driver under overshoot, a planning horizon of 50 years or more might be required before prospects of a long-term decline would start to affect adaptation decisions today or in the immediate future (Fig. 5a). Few adaptation plans and policies operate on such timescales: for example, the EU Adaptation Strategy spans three decades, while other national adaptation plans have similar or shorter time horizons<sup>43</sup>. Adaptation planning horizons and lifetimes of infrastructure can differ widely (Fig. 5b). At the long end of the planning scale, a hydropower dam may operate for a century or more, yet the management of that dam (and whether management should include flood control as an objective) would occur in concession periods (decades) as well as annual and sub-annual budget cycles (Fig. 5b).

The application of cost-benefit approaches in adaptation measures, and the time-scale over which these are assessed, requires decisions on intergenerational equity reflected in the choice of the intertemporal discount rate<sup>44</sup>. Higher discount rates limit the time horizon relevant for economic adaptation decision-making to a few decades (Fig. 5b).

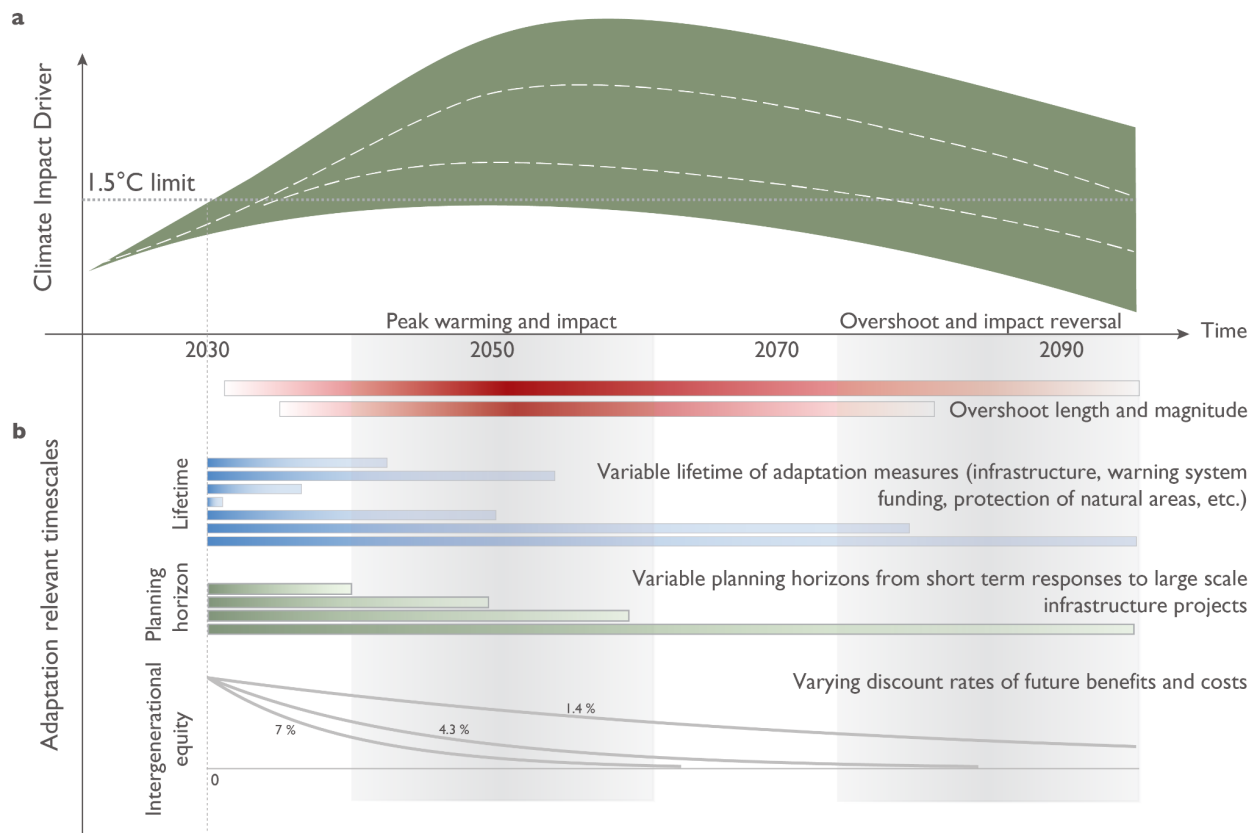


**Fig 5 | Adaptation relevant timescales and overshoot.** **a**, Stylised temporal evolution of a reversible climate impact driver under a peak-and-decline scenario. Dashed lines indicate a low and high overshoot outcome with timescales of GMT reversibility typically in line with those from the IPCC AR6 database. **b**, A stylised illustration of adaptation relevant timescales starting in 2030 including different lifetimes of individual adaptation measures (from years to decades, horizontal bars), the planning horizons for adaptation planning (decades) and the effect of applying discounting (reflecting societal preferences towards intergenerational equity) to future damages and adaptation benefits. We show the effect of discounting for three illustrative discount rates.

It therefore appears that long-term impact driver reversibility after overshoot may be of relevance only in specific cases of adaptation decision-making. A notable exception is adaptation against time-lagged irreversible impacts such as sea-level rise for which overshoots will affect the long-term outlook (Fig. 4). However, as we have shown above, long-term global temperature decline is nothing that can be relied on with certainty. Thus, a resilient adaptation strategy cannot be based on betting on overshoot.

Limits to adaptation, both soft and hard, constrain the option space available for adaptation<sup>39</sup>. This includes hard limits where, for example, adaptation is reliant on ecosystem-based measures that are themselves negatively impacted by climate change, as well as soft limits such as lack of resources or governance systems<sup>38</sup>. Transgressing hard

adaptation limits under overshoot by destroying sensitive ecosystems may render these measures unavailable under future warming reversal, reducing the available pool of adaptation measures compared to a no-overshoot case. The risk of transgressing adaptation limits, rather than uncertain prospects of long-term reversibility, appear to be most consequential for adaptation decision-making.

### **Reframing the overshoot discussion**

In this article, we argue that it is misleading to frame overshoot as an alternative way to achieving a similar climate outcome. We show that several climate impacts in a pre- and post-overshoot world are clearly different, indicating impact reversibility is not a given. Even in cases where impacts are reversible, the time scales for reversibility may be longer than typical decision horizons for adaptation planning, with peak warming impacts (as opposed to expected longer-term impacts) providing the backdrop for global adaptation needs assessments. From a climate justice perspective, overshoot entails further socio-economic impacts and climate-related loss and damage that are typically irreversible and fall most severely on the world's poor. This ethical dimension should be explicitly considered when assessing overshoot pathways and the possibilities to limit overshoot risks by near-term emissions reductions.

It has been argued that climate impacts during overshoots could be reduced or masked by the deployment of solar geoengineering (SG) intervention techniques<sup>45</sup> that would temporarily cool the planet. This idea is referred to as peak shaving. These suggestions, however, make strong assumptions about the applicability, effectiveness and governance of SG interventions. Accounting for uncertainties in the physical climate response, and in the evolution of future emissions after SG is deployed, implies that a SG intervention aimed at peak-shaving an overshoot could result in a multi-century commitment of both SG and CDR deployment<sup>23</sup>. In addition to fundamental concerns about SG deployment in isolation<sup>46</sup>, a peak-shaving discourse is prone to the same overconfidence in reversibility and effectiveness we have conceptualised in this article.

A central motivation to pursue a long-term temperature draw-down under PD scenarios is to reduce climate impacts. We have shown that such a temperature draw-down would indeed be effective in reducing the time-lagged impact emergence over centuries including sea-level rise and cryospheric changes. The consequences of multi-meter long-term sea level rise will affect coastal regions globally and drawing down global temperatures is important to minimise these long-term risks. Similarly, the probability of crossing irreversible

thresholds may remain substantial in the long-term unless global mean temperature is brought back down below 1°C above pre-industrial levels<sup>31</sup>.

Based on these insights, we argue for a reframing of the science and policy discourse on overshoot to focus on minimising climate risks in peak and decline temperature pathways (Table 1). We draw two overarching conclusions:

First, emissions reductions need to be accelerated as quickly as possible to slow down temperature increase and reduce peak warming. Pursuing such an *enhanced protection pathway* (Table 1) is the only robust strategy to at least minimise, if not avoid, far-reaching climate risks over the 21st century.

Second, we suggest that there is a need to prepare for an environmentally sustainable CDR capacity to hedge against long-term high-risk outcomes resulting from stronger than expected climate feedbacks. We find that such a preventive CDR capacity might need to be of the order of several hundred gigatonnes of cumulative NNCE, a scale that might be just about possible within sustainable limits of CDR deployment<sup>9</sup>. Designed as a preventive measure, this must not be planned to counterbalance residual emissions, leaving little room for CDR deployment for offsetting of residual emissions<sup>47</sup>. This further underscores the importance of very stringent near-term emission reductions to limit long-term risks<sup>48</sup>. Although we argue that the build up of a preventive CDR capacity is required to hedge against high warming outcomes, this same CDR capacity could, in case high warming outcomes can be ruled out with certainty, also be deployed to draw down long-term temperatures and thereby reduce climate risks.

The need for a preventive capacity has implications for the design of stringent emission reduction pathways in light of constraints that limit overall CDR deployment. Pathways relying on large amounts of CDR to even achieve net-zero CO<sub>2</sub> often exhaust or exceed sustainability limits by design<sup>15</sup>, leaving little to no room for course adjustments in case of high warming outcomes. On the other hand, pathways that do not plan for future development of CDR may fail to build up the technological solutions required to establish a preventive CDR capacity, thereby exposing future generations and in particular most vulnerable communities to risks that could at least be partly hedged against. Incorporating preventive CDR in pathway design requires further reflection, including regarding risks and policy design<sup>49</sup>, but also about how to assign responsibilities and incentivise different actors for providing for this preventive CDR capacity<sup>50</sup>.

As a consequence of ever-delayed emission reductions, there is a high chance of exceeding global warming of 1.5°C, and even 2°C, under emission pathways reflecting current policy ambitions<sup>1</sup>. Even if global temperatures are brought down below those levels in the long term, such an overshoot will come with irreversible consequences. Only stringent, immediate emission reductions can effectively limit climate risks.

## References

1. Rogelj, J. *et al.* Credibility gap in net-zero climate targets leaves world at high risk. *Science* **380**, 1014–1016 (2023).
2. IPCC. Summary for Policymakers. in *Climate Change 2022: Mitigation of Climate Change. Contribution of Working Group III to the Sixth Assessment Report of the Intergovernmental Panel on Climate Change* (eds. Shukla, P. R. *et al.*) (Cambridge University Press, Cambridge, UK and New York, NY, USA, 2022). doi:10.1017/9781009157926.001.
3. Prütz, R., Strefler, J., Rogelj, J. & Fuss, S. Understanding the carbon dioxide removal range in 1.5 °C compatible and high overshoot pathways. *Environ. Res. Commun.* **5**, 041005 (2023).
4. Schwinger, J., Asaadi, A., Steinert, N. J. & Lee, H. Emit now, mitigate later? Earth system reversibility under overshoots of different magnitudes and durations. *Earth Syst. Dyn.* **13**, 1641–1665 (2022).
5. Pfliederer, P., Schleussner, C.-F. & Sillmann, J. Limited reversal of regional climate signals in overshoot scenarios. (2023).
6. IPCC. Summary for Policymakers. *Climate Change 2021: The Physical Science Basis. Contribution of Working Group I to the Sixth Assessment Report of the Intergovernmental Panel on Climate Change* 3–32 (2021) doi:10.1017/9781009157896.001.
7. MacDougall, A. *et al.* Is there warming in the pipeline? A multi-model analysis of the zero emission commitment from CO<sub>2</sub>. *Biogeosciences* 1–45 (2020) doi:10.5194/bg-2019-492.
8. Smith, S. *et al.* The State of Carbon Dioxide Removal – 1st Edition. (2023).
9. Deprez, A. *et al.* Sustainability limits needed for CO<sub>2</sub> removal. *Science* **383**, 484–486 (2024).
10. Schneider, S. H. & Mastrandrea, M. D. Probabilistic assessment of “dangerous” climate change and emissions pathways. *Proc. Natl. Acad. Sci.* **102**, 15728–15735 (2005).
11. Wigley, T. M. L., Richels, R. & Edmonds, J. A. Economic and environmental choices in the stabilization of atmospheric CO<sub>2</sub> concentrations. *Nature* **379**, 240–243 (1996).
12. Azar, C., Johansson, D. J. A. & Mattsson, N. Meeting global temperature targets—the role of bioenergy with carbon capture and storage. *Environ. Res. Lett.* **8**, 034004 (2013).
13. Schleussner, C.-F. *et al.* Science and policy characteristics of the Paris Agreement temperature goal. *Nat. Clim. Change* **6**, 827–835 (2016).
14. Rajamani, L. & Werksman, J. The legal character and operational relevance of the Paris Agreement’s temperature goal. *Philos. Trans. R. Soc. Math. Phys. Eng. Sci.* **376**, (2018).
15. Riahi, K. *et al.* Chapter 3 Mitigation pathways compatible with long-term goals. in *IPCC, 2022: Climate*

*Change 2022: Mitigation of Climate Change. Contribution of Working Group III to the Sixth Assessment Report of the Intergovernmental Panel on Climate Change* (eds. Shukla, P. R. et al.) (Cambridge University Press, Cambridge, 2022). doi:10.1017/9781009157926.005.

16. Rogelj, J. *et al.* A new scenario logic for the Paris Agreement long-term temperature goal. *Nature* **573**, 357–363 (2019).
17. Schleussner, C.-F., Ganti, G., Rogelj, J. & Gidden, M. J. An emission pathway classification reflecting the Paris Agreement climate objectives. *Commun. Earth Environ.* **3**, 135 (2022).
18. Forster, P. *et al.* The Earth's Energy Budget, Climate Feedbacks, and Climate Sensitivity. *Climate Change 2021: The Physical Science Basis. Contribution of Working Group I to the Sixth Assessment Report of the Intergovernmental Panel on Climate Change* 923–1054 (2021) doi:10.1017/9781009157896.009.
19. Palazzo Corner, S. *et al.* The Zero Emissions Commitment and climate stabilization. *Front. Sci.* **1**, (2023).
20. Grassi, G. *et al.* Harmonising the land-use flux estimates of global models and national inventories for 2000–2020. *Earth Syst. Sci. Data* **15**, 1093–1114 (2023).
21. Meinshausen, M. *et al.* A perspective on the next generation of Earth system model scenarios: towards representative emission pathways (REPs). *Geosci. Model Dev. Discuss.* 1–40 (2023) doi:10.5194/gmd-2023-176.
22. Zickfeld, K., Azevedo, D., Mathesius, S. & Matthews, H. D. Asymmetry in the climate–carbon cycle response to positive and negative CO<sub>2</sub> emissions. *Nat. Clim. Change* **11**, 613–617 (2021).
23. Baur, S., Nauels, A., Nicholls, Z., Sanderson, B. M. & Schleussner, C.-F. The deployment length of solar radiation modification: an interplay of mitigation, net-negative emissions and climate uncertainty. *Earth Syst. Dyn.* **14**, 367–381 (2023).
24. Canadell, J. G. *et al.* Global Carbon and other Biogeochemical Cycles and Feedbacks. *Climate Change 2021: The Physical Science Basis. Contribution of Working Group I to the Sixth Assessment Report of the Intergovernmental Panel on Climate Change* 673–816 (2021) doi:10.1017/9781009157896.007.
25. McLaren, D., Willis, R., Szerszynski, B., Tyfield, D. & Markusson, N. Attractions of delay: Using deliberative engagement to investigate the political and strategic impacts of greenhouse gas removal technologies. *Environ. Plan. E Nat. Space* **6**, 578–599 (2023).
26. Powis, C. M., Smith, S. M., Minx, J. C. & Gasser, T. Quantifying global carbon dioxide removal deployment. *Environ. Res. Lett.* **18**, 024022 (2023).
27. Ruben Prütz, Sabine Fuss, Sarah Lück, Leon Stephan, & Joeri Rogelj. A new taxonomy to map evidence on carbon dioxide removal side effects. Preprint at <https://doi.org/10.21203/rs.3.rs-3697442/v1> (2023).
28. Stuart-Smith, R. F., Rajamani, L., Rogelj, J. & Wetzler, T. Legal limits to the use of CO<sub>2</sub> removal. *Science* **382**, 772–774 (2023).
29. Bellomo, K., Angeloni, M., Corti, S. & von Hardenberg, J. Future climate change shaped by inter-model differences in Atlantic meridional overturning circulation response. *Nat. Commun.* **12**, 3659 (2021).
30. Schwinger, J., Asaadi, A., Goris, N. & Lee, H. Possibility for strong northern hemisphere high-latitude cooling under negative emissions. *Nat. Commun.* **13**, 1095 (2022).
31. Wunderling, N. *et al.* Global warming overshoots increase risks of climate tipping cascades in a network model. *Nat. Clim. Change* **13**, 75–82 (2023).

32. Rugenstein, M. *et al.* LongRunMIP: Motivation and Design for a Large Collection of Millennial-Length AOGCM Simulations. *Bull. Am. Meteorol. Soc.* **100**, 2551–2570 (2019).
33. King, A. D. *et al.* Preparing for a post-net-zero world. *Nat. Clim. Change* **12**, 775–777 (2022).
34. Santana-Falcón, Y. *et al.* Irreversible loss in marine ecosystem habitability after a temperature overshoot. *Commun. Earth Environ.* **4**, 1–14 (2023).
35. Schleussner, C.-F. *et al.* Crop productivity changes in 1.5 °C and 2 °C worlds under climate sensitivity uncertainty. *Environ. Res. Lett.* **13**, 064007 (2018).
36. Meyer, A. L. S., Bentley, J., Odoulami, R. C., Pigot, A. L. & Trisos, C. H. Risks to biodiversity from temperature overshoot pathways. *Philos. Trans. R. Soc. B Biol. Sci.* **377**, 20210394 (2022).
37. Mengel, M., Nauels, A., Rogelj, J. & Schleussner, C.-F. Committed sea-level rise under the Paris Agreement and the legacy of delayed mitigation action. *Nat. Commun.* **9**, 601 (2018).
38. Andrijevic, M. *et al.* Towards scenario representation of adaptive capacity for global climate change assessments. *Nat. Clim. Change* 1–10 (2023) doi:10.1038/s41558-023-01725-1.
39. Thomas, A. *et al.* Global evidence of constraints and limits to human adaptation. *Reg. Environ. Change* **21**, 85 (2021).
40. Birkmann, J. *et al.* Poverty, Livelihoods and Sustainable Development. *Climate Change 2022: Impacts, Adaptation and Vulnerability. Contribution of Working Group II to the Sixth Assessment Report of the Intergovernmental Panel on Climate Change* 1171–1274 (2022) doi:10.1017/9781009325844.010.1171.
41. Burke, M., Hsiang, S. M. & Miguel, E. Global non-linear effect of temperature on economic production. *Nature* **527**, 235–239 (2015).
42. Parry, M., Lowe, J. & Hanson, C. Overshoot, adapt and recover. *Nature* **458**, 1102–1103 (2009).
43. National Adaptation Plans 2021. Progress in the formulation and implementation of NAPs | UNFCCC. <https://unfccc.int/documents/548662>.
44. Caney, S. Climate change, intergenerational equity and the social discount rate. *Polit. Philos. Econ.* **13**, 320–342 (2014).
45. MacMartin, D. G., Ricke, K. L. & Keith, D. W. Solar geoengineering as part of an overall strategy for meeting the 1.5°C Paris target. *Philos. Trans. R. Soc. Math. Phys. Eng. Sci.* **376**, (2018).
46. Biermann, F. *et al.* Solar geoengineering: The case for an international non-use agreement. *WIREs Clim. Change* **13**, e754 (2022).
47. Buck, H. J., Carton, W., Lund, J. F. & Markusson, N. Why residual emissions matter right now. *Nat. Clim. Change* **13**, 351–358 (2023).
48. Ho, D. T. Carbon dioxide removal is not a current climate solution — we need to change the narrative. *Nature* **616**, 9–9 (2023).
49. Bednar, J. *et al.* Operationalizing the net-negative carbon economy. *Nature* **596**, 377–383 (2021).
50. Fyson, C. L., Baur, S., Gidden, M. & Schleussner, C. Fair-share carbon dioxide removal increases major emitter responsibility. *Nat. Clim. Change* **10**, 836–841 (2020).

## Methods

### Evaluating net-negative CO<sub>2</sub> emissions needs reflecting climate uncertainty

In our illustrative analysis we assess the net-negative CO<sub>2</sub> emissions (NNCE) for the PROVIDE REN\_NZCO2 scenario<sup>51</sup>. The REN\_NZCO2 scenario follows the emission trajectory of the Illustrative Mitigation Pathway (IMP) “REN” from the IPCC’s 6th Assessment Report (AR6)<sup>52-54</sup> until the year of net-zero CO<sub>2</sub> (2060 for this scenario). After the year of net-zero CO<sub>2</sub>, emissions (of both GHGs and aerosol precursors) are kept constant.

#### *Deriving climate response metrics*

For this analysis we need to derive three metrics that capture different elements of the climate response during the warming phase and the long-term phase. These are:

1. The effective transient response to cumulative emissions (up), or eTCRE<sub>up</sub>: This metric captures the expected warming for a given quantity of cumulative emissions until net-zero CO<sub>2</sub>;
2. The effective transient response to cumulative emissions (down), or eTCRE<sub>down</sub>: This metric captures the expected warming or cooling for a given quantity of cumulative net-negative emissions after net-zero CO<sub>2</sub>. This is a purely diagnostic metric and incorporates also the effects of the effective Zero Emissions Commitment (eZEC).
3. The effective zero emissions commitment (eZEC): The continued temperature response after net-zero CO<sub>2</sub> emissions are achieved and sustained<sup>7</sup>. Here, eZEC is evaluated over 40 years (between 2060 and 2100).

To estimate eTCRE<sub>up</sub> (Equation 1), we directly use the warming outcomes reported in the PROVIDE ensemble. The warming outcomes are evaluated using the simple climate and carbon cycle model FaIR v.1.6.2<sup>55</sup> in a probabilistic setup with 2237 ensemble members consistent with the uncertainty assessment of IPCC AR6<sup>56</sup>. Each ensemble member has a specific parameter configuration that allows for the assessment of ensemble member specific properties like the climate metrics introduced above across different emission scenarios. This probabilistic setup of FaIR is consistent with assessed ranges of equilibrium climate sensitivity, historical global average surface temperature and other important metrics assessed by IPCC AR6 WG1<sup>18</sup>.

$$eTCRE_{up}(n) = \frac{T_{2060}(n) - T_{2000}(n)}{\sum_{2000}^{2060} E_{t'}} \quad (1)$$

Where,  $n$  refers to the ensemble member from FaIR,  $t'$  is the time step,  $E_{t'}$  is the net CO<sub>2</sub> emissions in time step  $t'$ , and  $T_{t'}(n)$  refers to the warming in the time step  $t'$  for a given ensemble member.

We need to take a different approach to estimating the second metric ( $eTCRE_{down}$ ), since the PROVIDE REN\_NZCO2 does not have NNCE by design. We adapt this scenario with different floor levels of NNCE ranging from 5 Gt CO<sub>2</sub>/yr to 25 Gt CO<sub>2</sub>/yr (Extended Data Fig. 1) that are applied from 2061 to 2100. The scenario is unchanged before 2060. We then calculate the warming outcomes for each of these scenarios applying the same probabilistic FaIR setup and identify the scenario (in this case, REN\_NZCO2 with 20 Gt CO<sub>2</sub>/yr net removals) for which all ensemble members are cooling between 2060 and 2100 (Extended Data Fig. 1). This is required to get an appropriate measure of NNCE emissions. From this adapted scenario, we evaluate the  $eTCRE_{down}$  for each ensemble member using Equation 2.

$$eTCRE_{down}(n) = \frac{T_{2100}(n) - T_{2060}(n)}{\sum_{2060}^{2100} E_{t'}} \quad (2)$$

#### *Calculating cumulative NNCE for each ensemble member*

Each ensemble member demonstrates a different level of peak warming that depends on  $eTCRE_{up}$  (Figure 2c). We calculate the cumulative NNCE (per ensemble member) that is necessary to ensure post-peak cooling to 1.5°C in 2100 using Equation 3 depending on the case:

$$NNCE(n) = 0 \text{ if } T_{2060}(n) < 1.5 \text{ else } \frac{1.5 - T_{2060}(n)}{eTCRE_{down}(n)} \quad (3)$$

Estimating the effective zero emissions commitment ( $eZEC$ ) allows us to separate the stabilisation and decline components of  $NNCE$ . We evaluate  $eZEC$  using the post-2060 warming outcome of the original PROVIDE REN\_NZCO2 scenario (Equation 4)

$$eZEC(n) = T_{2100}(n) - T_{2060}(n) \quad (4)$$

We assess the component of  $NNCE(n)$  to compensate for a positive  $eZEC$  using Equation (5).

$$NNCE_{stabilisation}(n) = 0 \text{ if } T_{2060}(n) < 1.5 \text{ else } \frac{eZEC(n)}{eTCRE_{down}(n)} \quad (5)$$

We then assess the component of this  $NNCE(n)$  for cooling after stabilisation using Equation (6).

$$NNCE_{decline}(n) = NNCE(n) - NNCE_{stabilisation}(n) \quad (6)$$

### *Estimating FaIR v1.6.2 ensemble member diagnostics for validation*

To evaluate the robustness of our NNCE estimates, we evaluate our FaIR model ensemble against the IPCC AR6 assessments for two key idealised model diagnostics, Equilibrium Climate Sensitivity (ECS) and the Zero Emissions Commitment (ZEC). ECS refers to the steady state change in the surface temperature following a doubling of the atmospheric CO<sub>2</sub> concentration from pre-industrial conditions<sup>57</sup>. ZEC is the global warming resulting after anthropogenic CO<sub>2</sub> emissions have reached zero and is determined by the balance between continued warming from past emissions and declining atmospheric CO<sub>2</sub> concentration that reduces radiative forcing after emissions cease<sup>7</sup>.

The ECS is defined<sup>58</sup> as

$$ECS = F_{2\times}/\lambda \quad (7)$$

where  $F_{2\times}$  is the effective radiative forcing from a doubling of CO<sub>2</sub> and  $\lambda$  is the climate feedback parameter.  $F_{2\times}$  and  $\lambda$  are parameters that are both used directly in FaIR, and therefore ECS can be calculated for each ensemble member.

We diagnose the ZEC for each ensemble member by performing the bell-shaped ZEC experiments from the ZECMIP modelling protocol (corresponding to the B1-B3 experiments from ref.<sup>7</sup>). These experiments are CO<sub>2</sub> only runs, with a bell-shaped emissions profile with a cumulative emissions constraint (750, 1000, and 2000 PgC respectively) applied over a 100 year time period from the beginning of the simulation period. All non-CO<sub>2</sub> forcings are fixed at pre-industrial levels. The ZEC<sub>50</sub> estimate per ensemble member is then calculated as the difference between the temperatures in year 150 and 100 of the simulation. This ZEC<sub>50</sub> estimate is purely used for diagnostic purposes and differs from our eZEC estimate, with the latter dependent on the specific characteristics of the emission pathway we apply. However, as the “bell” experiments approach zero emissions gradually from above and are somewhat similar to actual mitigation scenario emissions profiles, they are good analogues for eZEC.

As expected following the extended calibration of FaIR against AR6, we find very good agreement between the distribution of ECS and ZEC across members of the FaIR ensemble and the AR6 assessment (compare Extended Data Fig. 1 a,b). We also report agreement of the modelled historical warming across the ensemble compared to the observational record (Extended Data Fig. 1 d). Based on this evaluation, we cannot rule out high ECS/ZEC ensemble

members that drive the tail of our NNCE distribution (Extended Data Fig. 1 c). Yet, we find high NNCE outcomes also materialise for moderate-high ECS and ZEC outcomes.

### **Overshoot reversibility for annual mean temperature and precipitation**

To investigate the role of stabilisation and overshoot for regional reversibility, we use simulations of two different Earth system models that (1) stabilise GSAT at approximately 1.5 °C of global warming with respect to pre-industrial times, and (2) overshoot this level by around 1.5 °C. GFDL-ESM2M<sup>59,60</sup> simulations were performed using the Adaptive Emission Reduction Approach (AERA)<sup>61</sup>, which adapts CO<sub>2</sub>-fe emissions successively every five years to reach stabilisation (1.5 °C) and temporary overshoot (peak warming of 3.0 °C) levels, before returning and stabilising at 1.5 °C of global warming in the latter case. In this setup, the remaining CO<sub>2</sub>-fe emissions budget is determined every five years based on the relationship of past global anthropogenic warming and CO<sub>2</sub>-fe emissions simulated by the model. The remaining anthropogenic CO<sub>2</sub> emissions or removals are then computed assuming non-CO<sub>2</sub> and land use change emissions following the RCP 2.6. Future CO<sub>2</sub> emissions are then redistributed following a cubic polynomial function, constrained to smoothly reach any given temperature level. Details for the stabilisation case are given in the Adaptive Emission Reduction Approach model intercomparison simulation protocol<sup>62</sup>.

Simulations using NorESM2-LM<sup>63</sup> were performed following idealized emission trajectories including phases of positive and negative CO<sub>2</sub> emissions<sup>4</sup>. These simulations are emission-driven, meaning atmospheric CO<sub>2</sub> concentrations change in reaction to both CO<sub>2</sub> emissions and exchanges between the atmosphere and ocean or land. The only applied forcing is CO<sub>2</sub> emissions into the atmosphere, while land use and non-CO<sub>2</sub> greenhouse gas forcings remain at pre-industrial levels. The idealized cumulative emission trajectories adhere to the Zero Emissions Commitment Model Intercomparison Project (ZECMIP) protocol<sup>64</sup>. These emissions are represented as bell-shaped curves, with 50 years of increasing emissions followed by 50 years of decreasing emissions. Negative cumulative emission trajectories follow a similar pattern but with a negative sign. The reference "stabilisation" simulation has cumulative carbon emissions of 1500Pg during the first 100 years followed by zero emissions for 300 years. The reference simulation reaches global warming levels of approximately 1.7 °C in the long term. NorESM2-LM has a low transient climate response to cumulative emissions (TCRE) of 1.32KEgC<sup>-1</sup>. For the "overshoot" simulation, the emission

trajectory involves cumulative carbon emissions of 2500 Pg over the first 100 years, following the same emissions profile as the reference scenario but with higher emissions rates. It is followed by the application of CDR (in this case assumed as Direct Air Capture) removing 1000 Pg of cumulative carbon over the period of another 100 years. After negative emissions cease, it follows an extended phase of 200 years of zero emissions, such that the amount of cumulative carbon emissions is identical to the reference simulation for that period.

### *Regional averaging*

We compute spatially weighted regional averages for land or ocean regions following IPCC AR6 regions. WNEU corresponds to land grid-cells in western central Europe (WCE) and northern Europe (NEU). NAO45 corresponds to ocean grid-cells in the North Atlantic region above 45°N (see encircled area Fig. 3e,f) . AMZ and WAF are land regions.

### *Scaling with GMST*

In Fig. 3 we show surface air temperature (tas) anomalies divided by 31-year smoothed GMST anomalies for different regions. Anomalies are calculated with respect to 1850-1900.

### *Period differences and statistical significance*

When comparing period averages between two scenarios (e.g. Fig. 3) or at different times in the same scenario (Extended Data Fig.5-7) we compare the magnitude of the difference with random period differences of the same length in piControl simulations. If the difference exceeds the 95th percentile (or is below the 5th percentile) of differences found in piControl simulations we consider the difference as statistically significantly outside of internal climate variability. When  $n$  runs are available for the comparison of period averages we select sets  $2n$  random periods and compute the difference between the first half and the second half of these random sets to mimic ensemble differences.

### *CMIP6 analysis*

We analyse climate projections for the SSP5-34-OS and the SSP1-19 scenario by 12 Earth System models of the Coupled Model Intercomparison Project Phase 6<sup>65</sup>: CESM2-WACCM, CanESM5, EC-Earth3, FGOALS-g3, GFDL-ESM4, GISS-E2-1-G, IPSL-CM6A-LR, MIROC-ES2L, MIROC6, MPI-ESM1-2-LR, MRI-ESM2-0, UKESM1-0-LL.

We smooth GMT time series by applying a 31-year running average. In each simulation run we identify *peak warming* as the year where this smoothed GMT reaches its maximum. Next, we select the years before and after peak warming where the smoothed GMT is

closest to -0.1 and -0.2 K below peak warming. There is a substantial, model-dependent asymmetry in the average time between the rate of change in GMT before and after peak warming (see ref. <sup>5</sup> for an overview). In each run we average yearly temperatures and precipitation for the 31 years around the above described years of interest. Finally, for each ESM these 31-year periods are averaged over all available runs of the ESM and an ensemble median for the 12 ESMs is computed for the displayed differences.

### **2300 projections for sea-level rise, permafrost and peatland**

We project sea-level rise, permafrost and peatland carbon emissions with two sets of scenario ensembles as documented in ref <sup>37</sup>. Both sets of scenarios stabilise temperature rise below 2°C, with one set of scenarios achieving and maintaining the net-zero GHG emission objective of the Paris Agreement and the other set achieving net-zero CO<sub>2</sub> emissions only. Sea-level rise projections are taken from ref <sup>37</sup>, based on a combination of a reduced-complexity model of global-mean temperature with a component based simple sea-level model to evaluate the implications of different emission pathways on sea-level rise until 2300. We project carbon dynamics for permafrost and northern peatlands for the aforementioned scenario set using the permafrost module of the compact earth systems model OSCAR<sup>66</sup>, and a peatland emulator calibrated on previously published peatland intercomparison project<sup>67</sup>. The forcing data used to drive the permafrost and peatland modules are GMT change and the atmospheric CO<sub>2</sub> concentration change relative to pre-industrial levels. Firstly, we simulated the CO<sub>2</sub> fluxes and CH<sub>4</sub> fluxes from both permafrost and northern peatlands (see Fig S3 for the responses of individual components). Next, we computed the net climate effects of these two systems using the GWP\* following the method described in ref <sup>67</sup>. We use Equation 7 to derive the CO<sub>2</sub>-warming-equivalent emissions ( $E_{CO_2-we*}$ ) of the CH<sub>4</sub> emissions, taking into account the delayed response of temperature to past changes in the CH<sub>4</sub> emission rate:

$$E_{CO_2-we*} = GWP_H \times \left( r \times \frac{\Delta E_{CH_4}}{\Delta t} \times H + s \times E_{CH_4} \right) \quad (7)$$

Where  $\Delta E_{CH_4}$  is the change in the emission rate of  $E_{CH_4}$  over the  $\Delta t$  preceding years;  $E_{CH_4}$  is the CH<sub>4</sub> emission rate for the year under consideration;  $r$  and  $s$  are the weights given to the impact of changing the CH<sub>4</sub> emission rate and the impact of the CH<sub>4</sub> stock. Following ref <sup>67</sup>, we use  $\Delta t = 20$ . Because of the dependency on the emission's historical trajectory and carbon cycle feedbacks, the values of  $r$  and  $s$  are scenario-dependent. Here we use the  $r = 0.68$  and  $s = 0.32$  (the values used in ref <sup>67</sup> for RCP2.6), with  $H = 100$  years,  $GWP_{100}$  of 29.8 for permafrost and  $GWP_{100}$  of 27.0 for peatland<sup>18</sup>.

We then estimate the global temperature change ( $\Delta T$ ) due to permafrost and peatland CO<sub>2</sub> and CH<sub>4</sub> emissions as the product of the cumulative anthropogenic CO<sub>2</sub>-we emissions from permafrost and northern peatlands and the TCRE:

$$\Delta T_{\text{permafrost\&peatland}} = TCRE \times (\sum_{1861}^{2300} (E_{CO_2,2300} - E_{CO_2,pre}) + \sum_{1861}^{2300} (E_{CO_2-we^*,2300} - E_{CO_2-we^*,pre})) \quad (8)$$

Where  $E_{CO_2,2300}$  and  $E_{CO_2,pre}$  are CO<sub>2</sub> emission rates from permafrost and northern peatlands in 2300 and in the pre-industrial era, respectively;  $E_{CO_2-we^*,2300}$  and  $E_{CO_2-we^*,pre}$  are CO<sub>2</sub>-we\* due to permafrost and northern peatland CH<sub>4</sub> emissions in 2300 and in the pre-industrial era, respectively. For TCRE, we take the median value of 0.45°C per 1000 GtCO<sub>2</sub><sup>18</sup>.

### Data and Code availability

The scripts to replicate Fig. 2-5 are available here:

[https://gitlab.com/climateanalytics/2023\\_overshoot\\_perspective](https://gitlab.com/climateanalytics/2023_overshoot_perspective). The PROVIDEv1.2 scenario data used for Fig. 2 is available at <https://zenodo.org/record/5886912>. Data required to reproduce Fig. 3 can be found here: <https://esgf-data.dkrz.de/search/cmip6-dkrz/>. Data required to reproduce Fig. 4 is included in the repository.

### Competing interests

The authors declare no competing interests.

### Author contributions

CFS and QL conceived the study. CFS designed the study and wrote the first draft. JR and CFS designed Fig. 1, GG performed the analysis underlying Fig. 2 supported by ZN, CJS and JR, PP performed the analysis underlying Fig. 3, BZ, MM and TG performed the analysis underlying Fig. 4. FL conducted the GFDL ESM2M overshoot and stabilisation simulations with input from TLF. All authors contributed to the writing of the manuscript.

## Acknowledgements

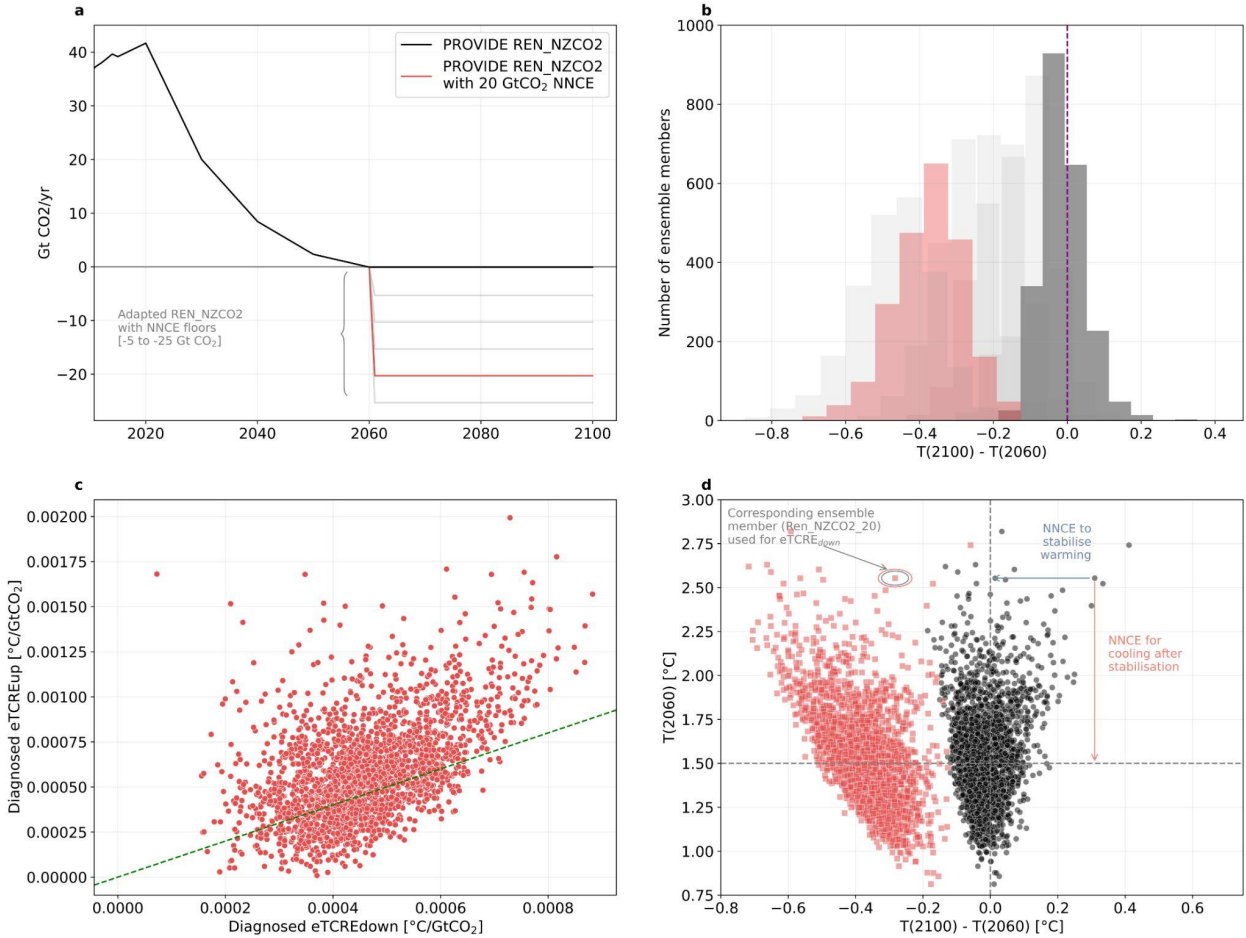
All authors acknowledge support from the European Union's Horizon 2020 research and innovation programmes under grant agreement No 101003687 (PROVIDE). GG acknowledges support from the Bundesministerium für Bildung und Forschung (BMBF) under grant agreement no. 01LS2108D (CDR PoEt). TG also acknowledges support from the European Union's Horizon 2020 and Horizon Europe research and innovation programmes under grant agreements #773421 (Nunataryuk) and #101056939 (RESCUE). JS is funded by the German Research Foundation (DFG) under Germany's Excellence Strategy—EXC 2037: "CLICCS— Climate, Climatic Change, and Society"—Project Number: 390683824, contribution to the Center for Earth System Research and Sustainability (CEN) of Universität Hamburg.

## References Methods

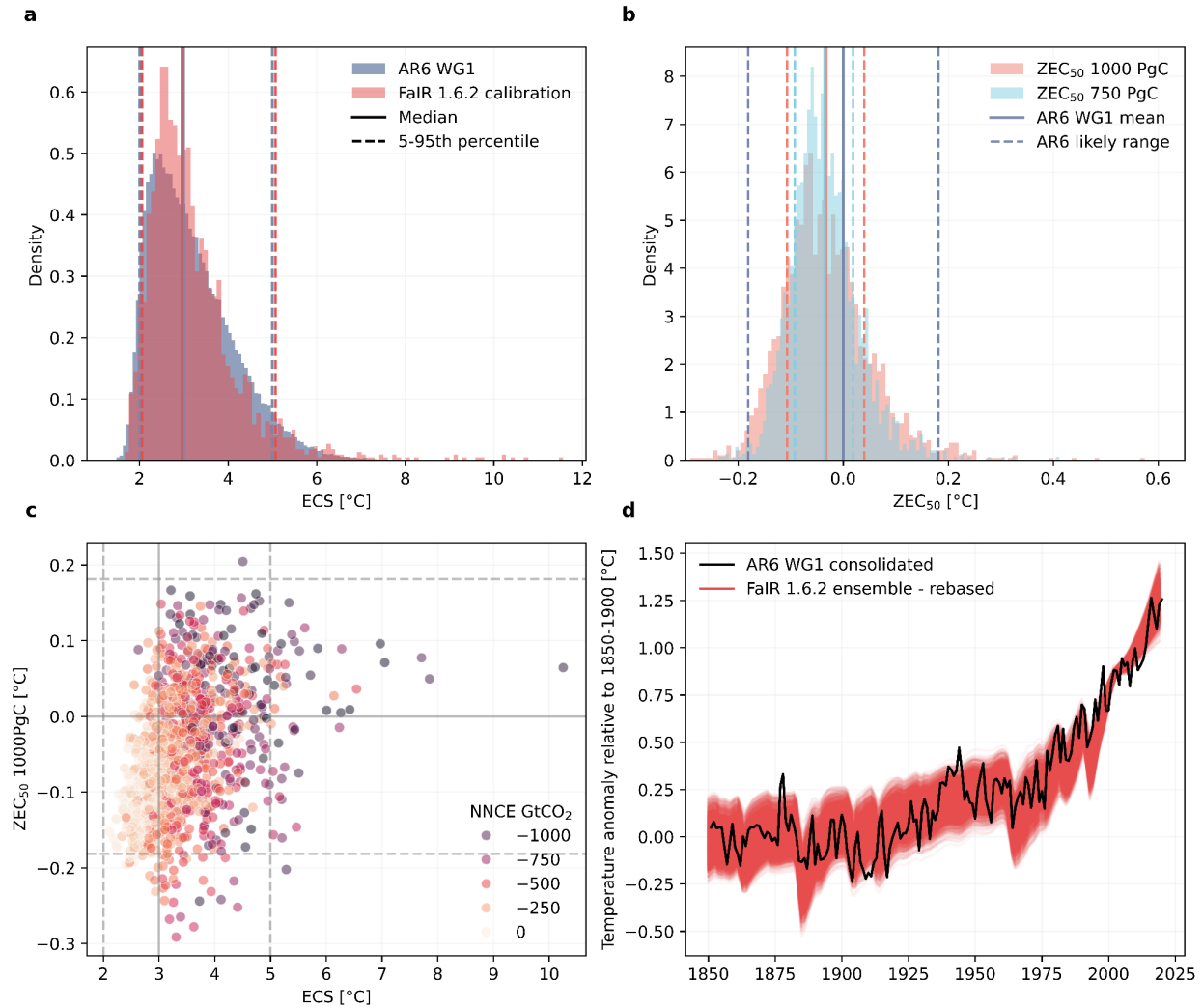
51. Lamboll, R., Rogelj, J. & Schleussner, C.-F. *A Guide to Scenarios for the PROVIDE Project*. <https://essopenarchive.org/doi/full/10.1002/essoar.10511875.2> (2022) doi:10.1002/essoar.10511875.2.
52. Luderer, G. *et al.* Impact of declining renewable energy costs on electrification in low-emission scenarios. *Nat. Energy* **7**, 32–42 (2022).
53. Riahi, K. *et al.* Mitigation pathways compatible with long-term goals. in *IPCC, 2022: Climate Change 2022: Mitigation of Climate Change. Contribution of Working Group III to the Sixth Assessment Report of the Intergovernmental Panel on Climate Change* (eds. Shukla, P. R. *et al.*) (Cambridge University Press, Cambridge, UK and New York, NY, USA, 2022). doi:10.1017/9781009157926.005.
54. Byers, E. *et al.* *AR6 Scenarios Database*. (2022) doi:10.5281/zenodo.5886912.
55. Smith, C. J. *et al.* FAIR v1.3: a simple emissions-based impulse response and carbon cycle model. *Geosci. Model Dev.* **11**, 2273–2297 (2018).
56. Nicholls, Z. *et al.* Cross-Chapter Box 7.1: Physical emulation of Earth System Models for scenario classification and knowledge integration in AR6. in *Climate Change 2021: The Physical Science Basis. Contribution of Working Group I to the Sixth Assessment Report of the Intergovernmental Panel on Climate Change* (eds. Masson-Delmotte, V. *et al.*) (Cambridge University Press, 2021).
57. IPCC. Annex VII: Glossary [Matthews, J.B.R., V. Möller, R. van Diemen, J.S. Fuglestvedt, V. Masson-Delmotte, C. Méndez, S. Semenov, A. Reisinger (eds.)]. *Climate Change 2021: The Physical Science Basis. Contribution of Working Group I to the Sixth Assessment Report of the Intergovernmental Panel on Climate Change* 2215–2256 (2021) doi:10.1017/9781009157896.022.
58. Sherwood, S. *et al.* An assessment of Earth's climate sensitivity using multiple lines of evidence. *Rev. Geophys.* **n/a**, e2019RG000678-e2019RG000678 (2020).
59. Dunne, J. P. *et al.* GFDL's ESM2 Global Coupled Climate–Carbon Earth System Models. Part II: Carbon System Formulation and Baseline Simulation Characteristics\*. *J. Clim.* **26**, 2247–2267 (2013).
60. Burger, F. A., John, J. G. & Frölicher, T. L. Increase in ocean acidity variability and extremes under increasing atmospheric CO<sub>2</sub>. *Biogeosciences* **17**, 4633–4662 (2020).
61. Terhaar, J., Frölicher, T. L., Aschwanden, M. T., Friedlingstein, P. & Joos, F. Adaptive emission reduction approach to reach any global warming target. *Nat. Clim. Change* **12**, 1136–1142 (2022).
62. Frölicher, T. L., Jens, T., Fortunat, J. & Yona, S. Protocol for Adaptive Emission Reduction Approach (AERA) simulations. (2022) doi:10.5281/zenodo.7473133.
63. Seland, Ø. *et al.* Overview of the Norwegian Earth System Model (NorESM2) and key climate response of CMIP6 DECK, historical, and scenario simulations. *Geosci. Model Dev.* **13**, 6165–6200 (2020).

64. Jones, C. D. *et al.* The Zero Emissions Commitment Model Intercomparison Project (ZECMIP) contribution to C4MIP: quantifying committed climate changes following zero carbon emissions. *Geosci. Model Dev.* **12**, 4375–4385 (2019).
65. O'Neill, B. C. *et al.* The Scenario Model Intercomparison Project (ScenarioMIP) for CMIP6. *Geosci. Model Dev. Discuss.* 1–35 (2016) doi:10.5194/gmd-2016-84.
66. Quilcaille, Y., Gasser, T., Ciais, P. & Boucher, O. CMIP6 simulations with the compact Earth system model OSCAR v3.1. *Geosci. Model Dev.* **16**, 1129–1161 (2023).
67. Qiu, C. *et al.* A strong mitigation scenario maintains climate neutrality of northern peatlands. *One Earth* **5**, 86–97 (2022).
68. Lane, J., Greig, C. & Garnett, A. Uncertain storage prospects create a conundrum for carbon capture and storage ambitions. *Nat. Clim. Change* **11**, 925–936 (2021).
69. Fuss, S. *et al.* Negative emissions—Part 2: Costs, potentials and side effects. *Environ. Res. Lett.* **13**, 063002 (2018).
70. Anderegg, W. R. L. *et al.* Climate-driven risks to the climate mitigation potential of forests. *Science* **368**, (2020).
71. Heikkinen, J., Keskinen, R., Kostensalo, J. & Nuutinen, V. Climate change induces carbon loss of arable mineral soils in boreal conditions. *Glob. Change Biol.* **28**, 3960–3973 (2022).
72. Chiquier, S., Patrizio, P., Bui, M., Sunny, N. & Dowell, N. M. A comparative analysis of the efficiency, timing, and permanence of CO<sub>2</sub> removal pathways. *Energy Environ. Sci.* **15**, 4389–4403 (2022).
73. Mengis, N., Paul, A. & Fernández-Méndez, M. Counting (on) blue carbon—Challenges and ways forward for carbon accounting of ecosystem-based carbon removal in marine environments. *PLOS Clim.* **2**, e0000148 (2023).
74. Jones, C. D. *et al.* Simulating the Earth system response to negative emissions. *Environ. Res. Lett.* **11**, 095012 (2016).
75. Realmonte, G. *et al.* An inter-model assessment of the role of direct air capture in deep mitigation pathways. *Nat. Commun.* **10**, 3277 (2019).
76. Krause, A. *et al.* Large uncertainty in carbon uptake potential of land-based climate-change mitigation efforts. *Glob. Change Biol.* **24**, 3025–3038 (2018).
77. Minx, J. C. *et al.* Negative emissions—Part 1: Research landscape and synthesis. *Environ. Res. Lett.* **13**, 063001–063001 (2018).
78. Grant, N., Hawkes, A., Mittal, S. & Gambhir, A. Confronting mitigation deterrence in low-carbon scenarios. *Environ. Res. Lett.* **16**, 64099–64099 (2021).
79. Carton, W., Hougaard, I.-M., Markusson, N. & Lund, J. F. Is carbon removal delaying emission reductions? *WIREs Clim. Change* **14**, e826 (2023).
80. Lee, K., Fyson, C. & Schleussner, C. F. Fair distributions of carbon dioxide removal obligations and implications for effective national net-zero targets. *Environ. Res. Lett.* **16**, (2021).
81. Gidden, M. J. *et al.* Aligning climate scenarios to emissions inventories shifts global benchmarks. *Nature* **624**, 102–108 (2023).
82. Yuwono, B. *et al.* Doing burden-sharing right to deliver natural climate solutions for carbon dioxide removal. *Nat.-Based Solut.* **3**, 100048 (2023).

# Extended Data



**Extended Data Fig. 1 | Method to derive net-negative CO<sub>2</sub> emissions under climate uncertainty for PROVIDE REN\_NZCO<sub>2</sub>.** **a**, The original PROVIDE REN\_NZCO<sub>2</sub> scenario (black) and the adapted PROVIDE REN\_NZCO<sub>2</sub> scenarios with different levels of net-negative CO<sub>2</sub> emissions. **b**, The difference between 2100 warming and 2060 warming across the scenarios. Estimates to the right of the purple line indicate ongoing warming after 2060. **c**, Diagnosed eTCREup and eTCREdown (estimated from PROVIDE REN\_NZCO<sub>2</sub>\_20), **d**, Cooling between 2100 and 2060 versus warming in 2060 for PROVIDE REN\_NZCO<sub>2</sub> and PROVIDE REN\_NZCO<sub>2</sub>\_20.

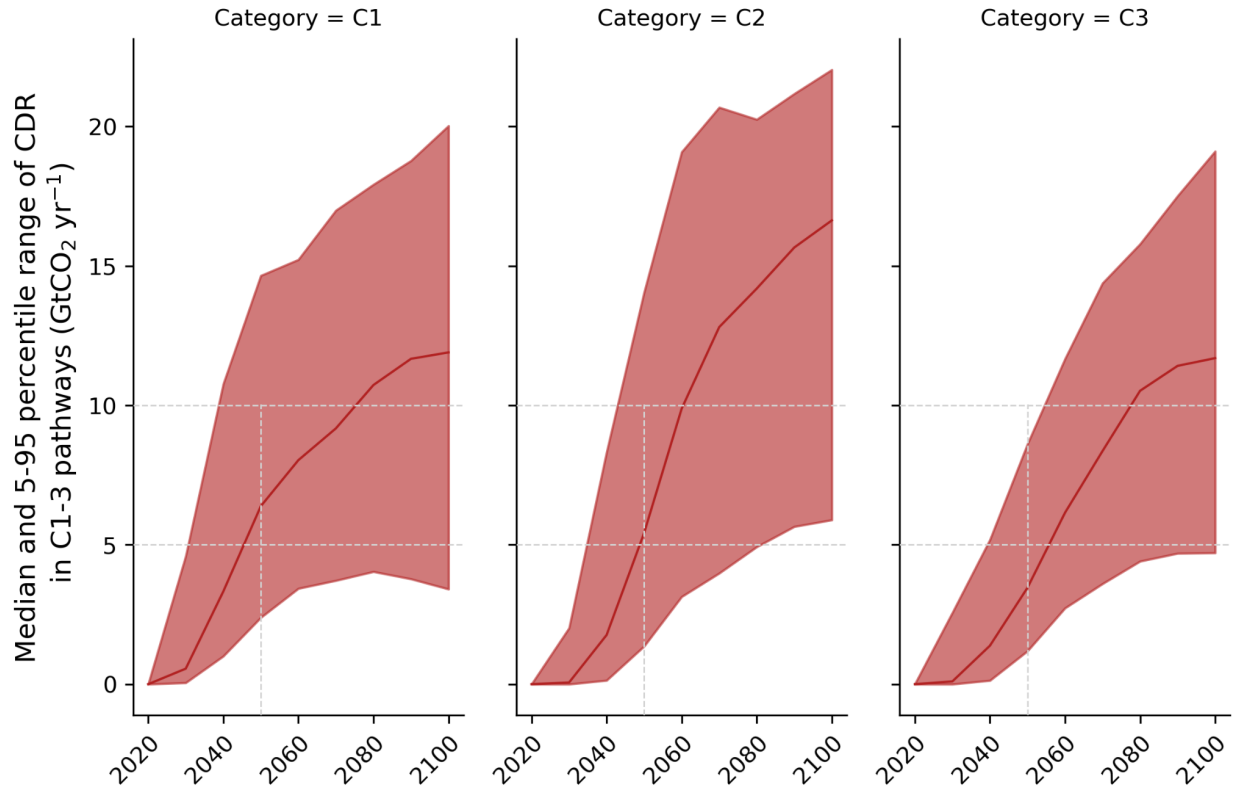


**Extended Data Figure 2 | FaIR v1.6.2 ensemble diagnostics consistent with AR6 WG1 assessment.** **a**, Equilibrium Climate Sensitivity (ECS), **b** Zero Emissions Commitment (ZEC) over a 50 year period after CO<sub>2</sub> emissions reach zero, **c** High ZEC and ECS drive high net-negative CO<sub>2</sub> emissions estimates in ensemble members. Solid and dashed horizontal (vertical) lines indicate the median and 5-95% for ZEC (ECS) distributions as in panel **a**,**b**, respectively. **d**, Consistency of FaIR ensemble members with the consolidated AR6 WG1 historical warming time series.

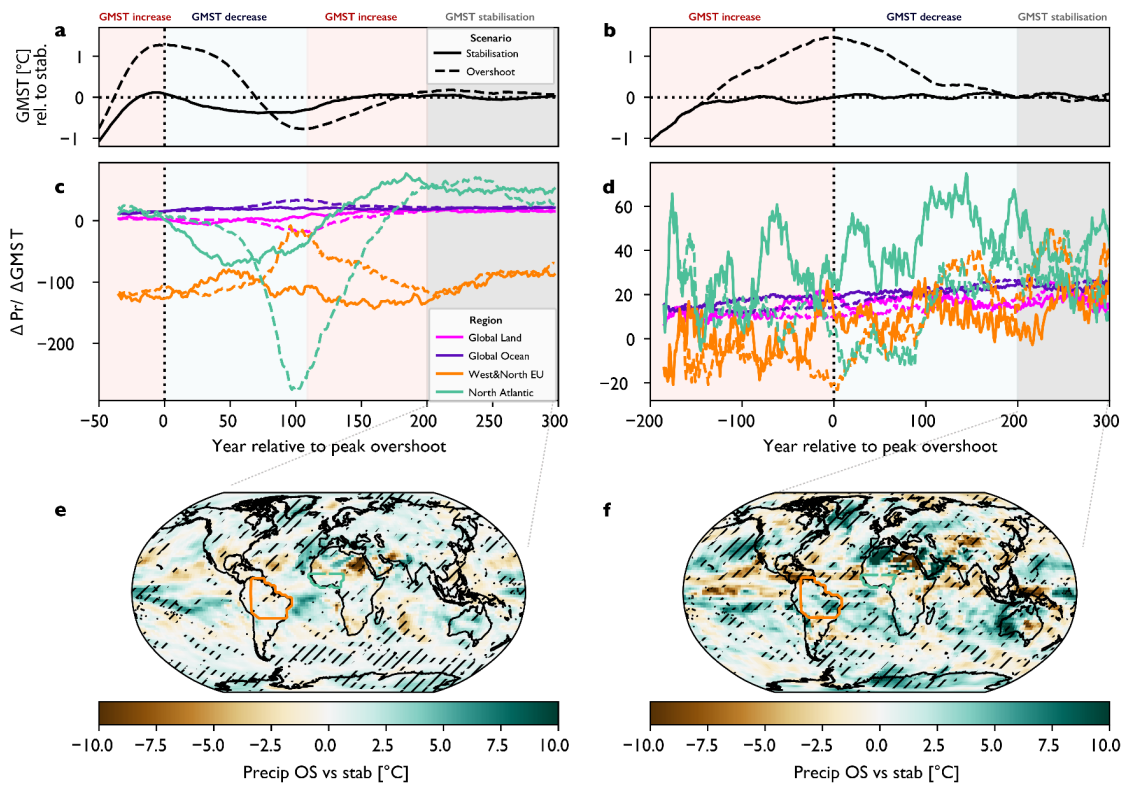
**Extended Data Table 1 | Overview of constraints of large-scale CDR**

	Description of constraints and potential for overconfidence
<b>Readiness</b>	Current removal capacities are far from what is required to be compatible with the Paris Agreement. In the coming years, removal scales need to go up while costs need to come down – both at highly ambitious levels. Implementation gaps already arise, potentially precluding reliance on CDR to steer back from overshoot <sup>8</sup> .

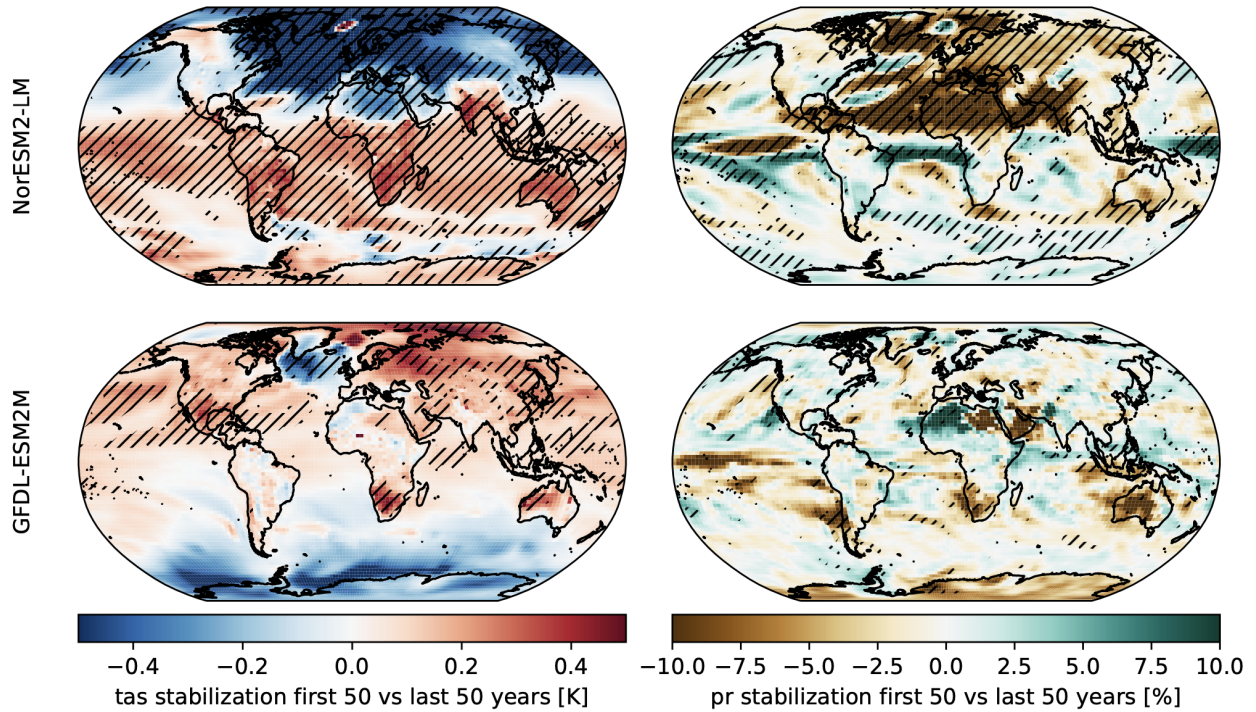
<p><b>Permanence &amp; resilience</b></p>	<p>Permanent and secure storage of removed carbon is key. Overconfidence may arise from neglected uncertainty of the geological storage potential<sup>68</sup> and overestimated storage durability of land and ocean sinks under progressing climate change. Carbon stored in soils and vegetation is especially susceptible to climate or non-climatic impacts, including fires or pest infestation, and may be constrained further if total sequestration potentials are lower than current best estimates<sup>69-72</sup>. Carbon sequestration in marine ecosystems is equally vulnerable to climate impacts<sup>73</sup>.</p>
<p><b>System feedbacks</b></p>	<p>Mitigation effects of CDR may be offset by weakened and potentially reversed land and ocean carbon sinks, and other undesired system feedbacks<sup>74</sup>, e.g., unfavourable albedo changes, or emissions due to direct or (unintended) indirect land use change. Carbon uptake potential of land-based CDR is highly uncertain, depending on bioenergy crop yields in the case of bioenergy and carbon capture and storage (BECCS) and soil carbon response to land-use change and the rate of forest regrowth in the case of afforestation<sup>75,76</sup>.</p>
<p><b>Policy response &amp; governance</b></p>	<p>Betting on CDR effectiveness may lead to insufficient emission reductions if CDR underperforms, or physical climate feedbacks are stronger than expected. The outlook of potential future CDR availability could deter mitigation, meaning that required gross emission reductions may be delayed and/or weakened<sup>25,77</sup> - an effect that can also be observed in integrated assessment models<sup>78,79</sup>. Lacking monitoring and liability of removal additionality and permanence may pose an additional constraint<sup>8</sup>.</p>
<p><b>Sustainability &amp; Acceptability</b></p>	<p>The extensive land use footprint associated with large-scale CDR may threaten environmental integrity<sup>70,71</sup> and/or agricultural production<sup>69</sup>. However, some types of CDR (for example, via restoration of natural ecosystems and their associated carbon) would be more synergistic. CDR often requires public acceptance – an aspect not reflected in current scenarios. Consensus is critical, as CDR can lead to undesired distributional impacts (e.g., concerning land tenure or food prices if large areas are allocated for CDR). Further constraints arise when considering (transnational) equity criteria, as the burden of CDR may not be evenly distributed between polluters, regions, and generations<sup>50,80</sup>. Even with strong CDR deployment by high-income countries, equitable mitigation outcomes may not be achieved<sup>81,82</sup>.</p>



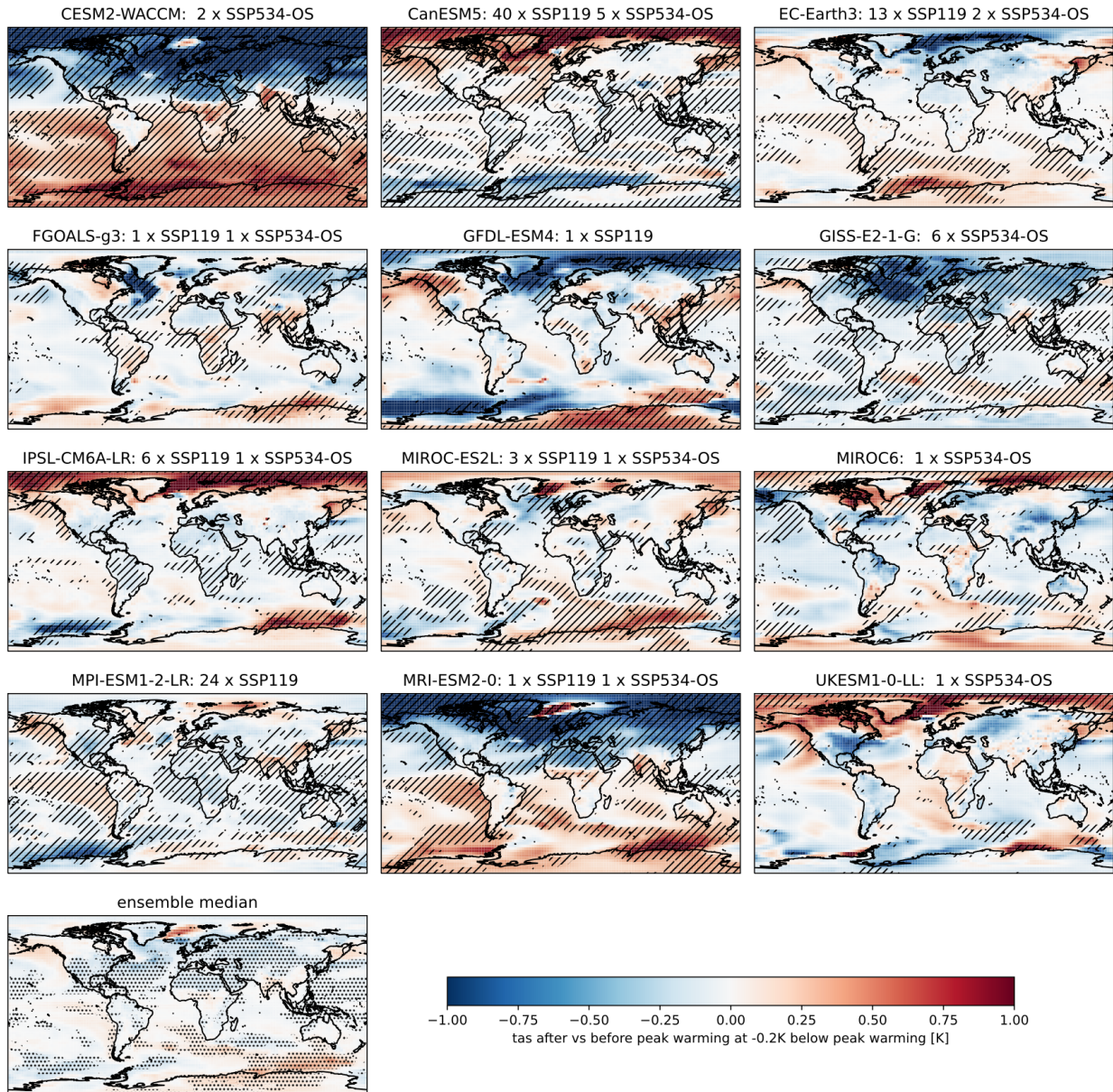
**Extended Data Figure 3 | Median carbon dioxide removal ranges in AR6 for 2020-2100 across C1-3 with 5-95 percentile ranges.** The figure includes BECCS, DACCS, enhanced weathering, net-removal from AFOLU and 'other' CDR. Net-removal from AFOLU is used as conservative proxy for land use sequestration to account for reporting inconsistencies for this variable.



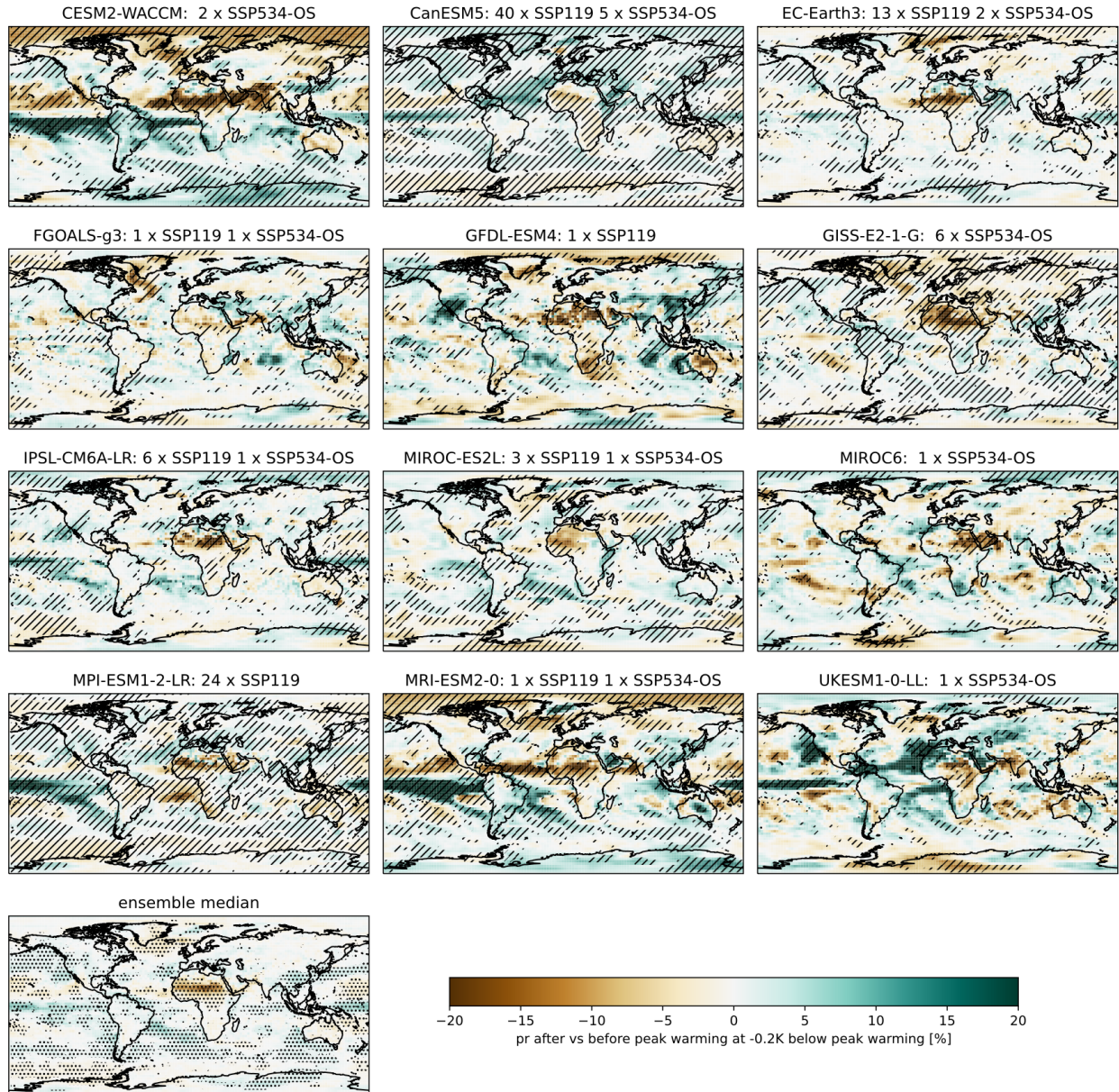
**Extended Data Figure 4 | Evolution of regional precipitation before and after overshoot compared to global temperature stabilisation. a ,c,e** show results for the NorESM Earth System Model, **b,d,f** for GFDL-ESM2M. **a,b** Global mean surface air temperature (GMT) trajectories for dedicated climate stabilisation (solid) and overshoot (dashed) scenarios. **c,d** temporal evolution of scaling coefficients of regional precipitation with GMT in for the global land and ocean areas as well as the Amazon and the West Africa region. **e,f** regional differences in annual precipitation between overshoot and stabilisation scenarios over hundred years of long-term GMT stabilisation (grey shaded area in panels **a,b**, hatching highlights grid-cells where the difference exceeds the 95th percentile (is below the 5th percentile) of comparable period differences in piControl simulations (Methods).



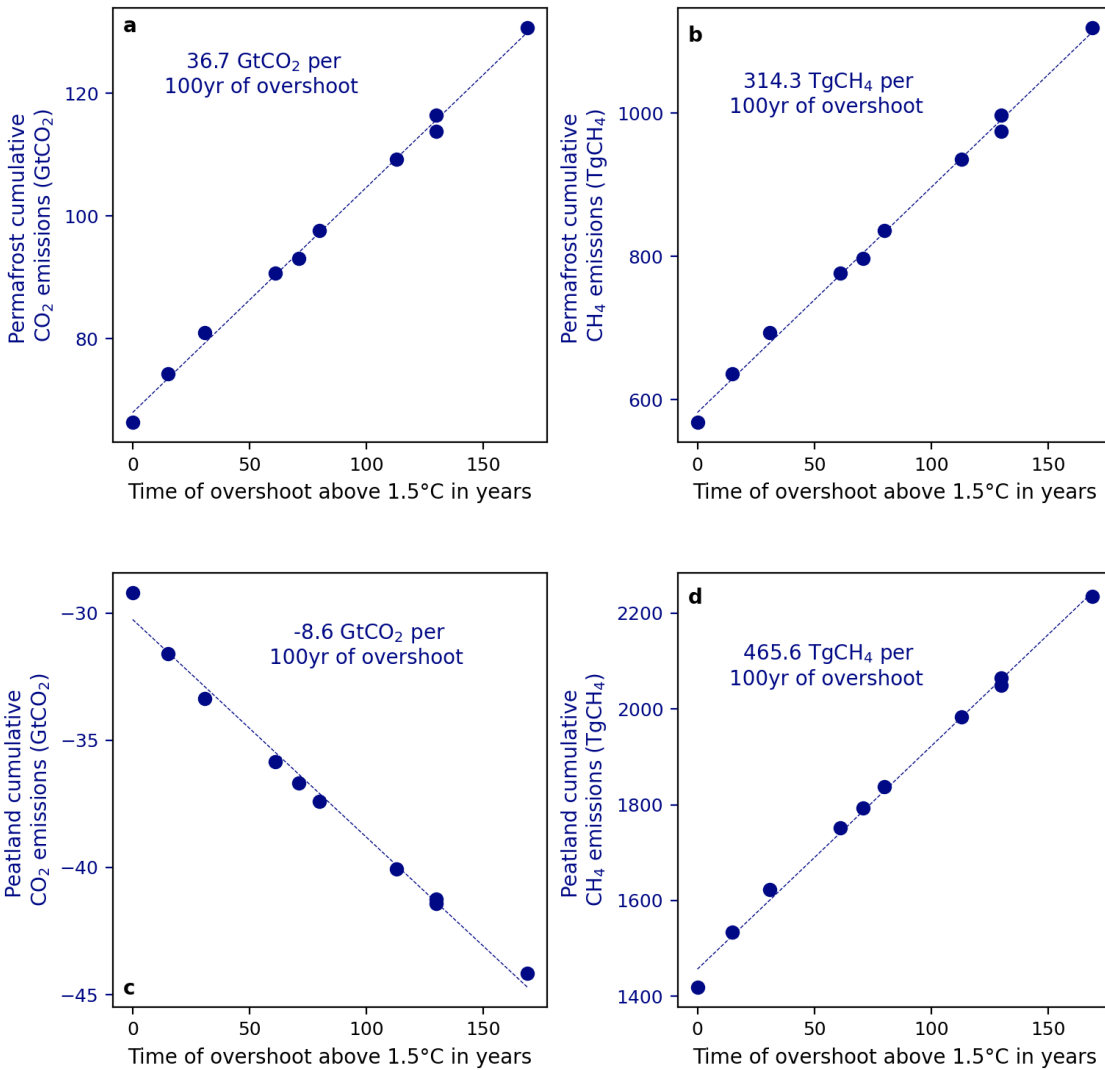
**Extended Data Figure 5 | Transient regional differences in a GMT stabilisation scenario. a,b** show results for NorESM, **c,d** for GFDL-ESM2M, **a,c** for annual temperature over the first 50 years of GMT stabilisation vs. the last 50 years (compare Fig. 3a). **c,d** like **a,c** but for annual precipitation. Hatching highlights grid-cells where the difference exceeds the 95th percentile (is below the 5th percentile) of comparable period differences in piControl simulations (Methods).



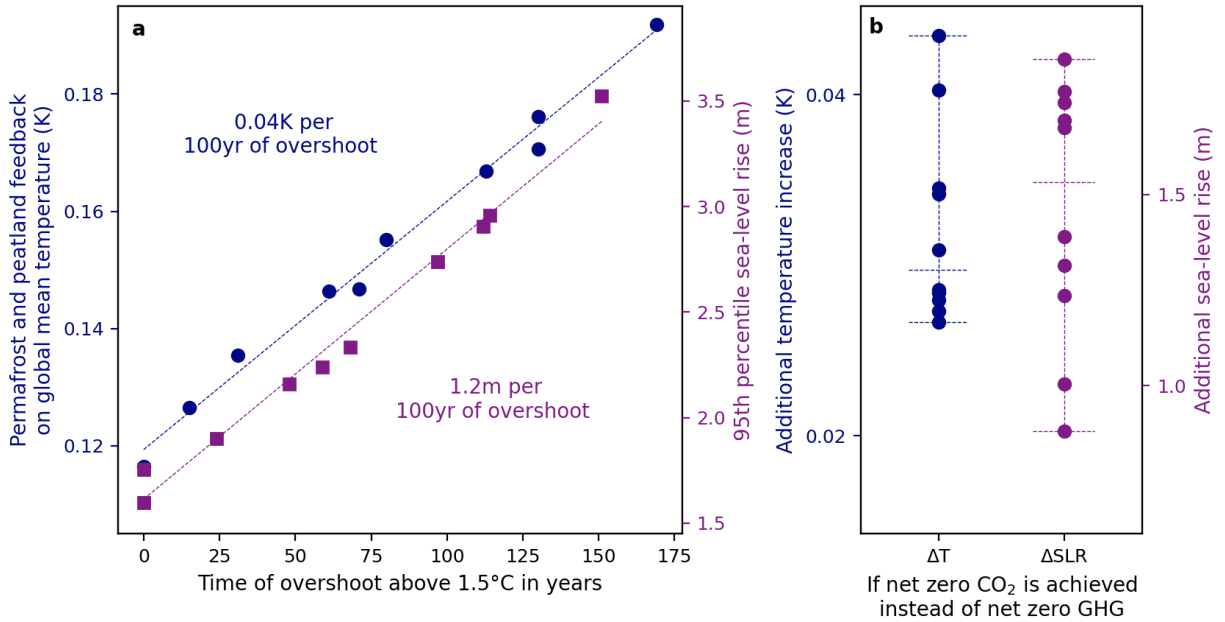
**Extended Data Figure 6 | Differences between regional annual temperature before and after overshoot in a CMIP6 model ensemble.** Patterns are shown for centred 31yr periods for GMT of  $-0.2^{\circ}\text{C}$  below peak warming before and after overshoot in the SSP5-34-OS and the SSP1-19 pathways (Methods). In the first 12 panels hatching highlights grid-cells where the difference exceeds the 95th percentile (is below the 5th percentile) of comparable period differences in piControl simulations (see methods). For the ensemble median (last panel) stippling indicates a model agreement in the sign of change of at least 66%.



**Extended Data Figure 7 | Differences between regional annual precipitation before and after overshoot in a CMIP6 model ensemble.** Patterns are shown for centred 31yr periods for GMT of  $-0.2^{\circ}\text{C}$  below peak warming before and after overshoot in the SSP5-34-OS and the SSP1-19 pathways (Methods). In the first 12 panels hatching highlights grid-cells where the difference exceeds the 95th percentile (is below the 5th percentile) of comparable period differences in piControl simulations (see methods). For the ensemble median (last panel) stippling indicates a model agreement in the sign of change of at least 66%.



**Extended Data Figure 8 | CO<sub>2</sub> and CH<sub>4</sub> emissions from permafrost and peatlands under overshoot. a,** Cumulative CO<sub>2</sub> emissions permafrost emissions as a function of length above 1.5°C. **b,** CH<sub>4</sub> emissions from permafrost. **c,** CO<sub>2</sub> emissions from peatlands. **d,** CH<sub>4</sub> emissions from permafrost.



**Extended Data Figure 9 | High-end long-term irreversible permafrost, peatland and sea-level rise impacts of overshoot.** As Fig. 4, but for the 95% quantile outcomes. **a**, Feedback on 2300 global mean temperature increase by permafrost and peatland emissions (blue markers and left axis) and 2300 global median sea-level rise (right axis) as a function of overshoot duration. Note that while the vertical axis provides 95% quantile outcomes, the overshoot length on the horizontal axis refers to the median overshoot length under a given scenario as in Fig. 4 to allow for direct comparability. **b**, Additional global mean temperature from warming-induced permafrost and peatland emissions and sea-level rise increase implied by stabilising temperatures at peak warming by achieving net-zero CO<sub>2</sub> emissions compared to a long-term temperature decline implied by achieving and maintaining net-zero GHGs.